Chapter 5
Cylindrical Shells

Cylindrical shells are the simplest case of shells of revolution. A cylindrical shell is formed by revolving a straight line (generator) around an axis that is paralleled to the line itself. The surface obtained from the revolution of the generator defined the cylindrical shell's middle surface. Cylindrical shells may have different geometrical shapes determined by the revolution routes and circumferential included angles. By appropriately selecting the revolution routes, cylindrical shells with desired cross-sections can be produced, such as circular, elliptic, rectangular, polygon, etc. In the literature and engineering applications, cylindrical shells with circular cross-sections are most frequently encountered. In this type of cylindrical shells, each point on the middle surface maintains a similar distance from the axis. The current chapter is devoted to dealing with closed and open circular cylindrical shells.

In recent decades, composite materials have found increasing application with the rapid development of industries because they offer advantages over conventional materials. As one of the important structural components, composite laminated circular cylindrical shells are widely used in various engineering applications, such as naval vehicles aircrafts, and civil industries. The vibration analysis of them is often required and has always been one important research subject in dynamic behaviors and optimal design of complex composite shells. The literature on the vibration analysis of cylindrical shells is vast. A large variety of classical and modern theories and different computational methods have been proposed by researchers, and extensive studies have been carried out based on these theories and methods. There are mainly three major theories which are usually known as: the classical shell theories (CSTs), the first-order shear deformation theories (FSDTs) and the higher-order shear deformation theories (HSDTs). The CSTs are based on the Kirchhoff–Love assumptions, in which transverse normal and shear deformations are neglected. Unlike thin plates, where only one theory (i.e., classical plate theory) is agreed upon by most researchers, thin shells have a variety of subcategory thin shell theories developed through different assumptions and simplifications, such as Reissner-Naghdi's linear shell theory, Donner-Mushtari's theory, Flügge's theory, Sanders' theory, etc., about which detailed descriptions are

G. Jin et al., *Structural Vibration*, DOI 10.1007/978-3-662-46364-2_5

available in the monograph by Leissa (1973). Many of the previous studies regarding laminated cylindrical shells are based on the CSTs (for example, Jin et al. 2013a; Lam and Loy 1995a, b, 1998; Liu et al. 2012; Qu et al. 2013c; Zhang 2001, 2002).

Although sufficiently accurate vibration results for thin shells can be achieved using the CSTs with appropriate solution procedures, they are inadequate for the vibration analysis of composite laminated shells which are rather thick or when they are made from materials with a high degree of anisotropic. In such cases, the effects of transverse shear deformations must be considered. Thus, FSDTs based on Reissner-Mindlin's displacement assumptions were developed to take into account the effects of transverse shear deformations. There exist considerable research efforts devoted to the laminated cylindrical shells based on the FSDTs (such as, Ferreira et al. 2007; Jin et al. 2013b, 2014a; Khdeir 1995; Khdeir and Reddy 1989; Qatu 1999; Qu et al. 2013a, b; Reddy 1984; Soldatos and Messina 2001; Zenkour 1998; Zenkour and Fares 2001; Ye et al. 2014b).

Since the transverse shear strains in the conventional FSDTs are assumed to be constant through the thickness, shear correction factors have to be incorporated to adjust the transverse shear stiffness. To overcome the deficiency of the FSDTs and further improve the dynamic analysis of shell structures, a number of HSDTs with varying degree of refinements of the kinematics of deformation were developed. Noticeably, significant contributions to the higher order shear deformation theories of composite shells have been made recently by many researchers (Ferreira et al. 2006; Mantari et al. 2011; Pinto Correia et al. 2003; Reddy and Liu 1985; Schmidt and Reddy 1988; Viola et al. 2012, 2013). As pointed out by Reddy (2003), although the HSDTs are capable of solving the global dynamic problem of shells more accurately, they introduce rather sophisticated formulations and boundary terms that are not easily applicable or yet understood. And these theories require more computational demanding compared to those FSDTs. Therefore, such theories should be used only when necessary. When the main emphasis of the analysis is to determine the vibration frequencies and mode shapes, the FSDTs may be a recommendable compromise between the solution accuracy and effort.

The development of researches on this subject has been well documented in several monographs respectively by Carrera et al. (2011), Qatu (2004), Reddy (2003), Ye (2003), Soedel (2004) and reviews (Carrera 2002, 2003; Liew et al. 2011; Qatu 2002a, b; Qatu et al. 2010; Toorani and Lakis 2000).

This chapter considers vibrations of laminated circular cylindrical shells with general boundary conditions. Equations of thin (classical shell theory, CST) and thick (shear deformation shell theory, SDST) laminated cylindrical shells are given in the first and second sections, respectively, by specializing the corresponding equations of the general shells (Chap. 1) to those of cylindrical shells. On the basis of SDST, several vibration results are presented for closed laminated cylindrical shells with different boundary conditions, lamination schemes and geometry

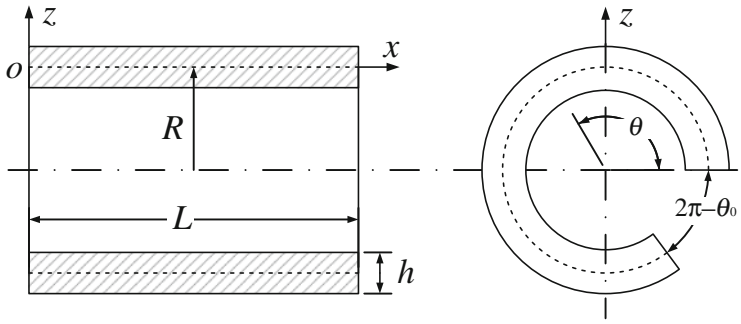

Fig. 5.1 Geometry notations and coordinate system of open laminated circular cylindrical shells

parameters by using the modified Fourier series and weak form solution procedure developed in Chap. 2 (Table 3.3 shows that convergence of solutions with weak form solution procedure is faster than the strong form one). Effects of boundary conditions, geometry parameters and material properties are studied as well. Vibration of shallow and deep open laminated cylindrical shells will then be treated in the latest section of this chapter.

Closed cylindrical shells are special cases of the open ones. Consider an open laminated circular cylindrical shell as shown in Fig. 5.1. The length, mean radius, total thickness and circumferential included angle of the shell are represented by L, R, h and θ_0, respectively. The middle surface of the shell where an orthogonal coordinate system (x, θ and z) is fixed is taken as the reference surface of the shell. The x, θ and z axes are taken in the axial, circumferential and radial directions accordingly. The middle surface displacements of the shell in the axial, circumferential and radial directions are denoted by u, v and w, respectively. The shell is assumed to be composed of arbitrary number of liner orthotropic laminas which are perfectly bonded together. The principal coordinates of the composite material in each layer are denoted by 1, 2 and 3, respectively, and the angle between the material axis and the x-axis of the shell is devoted by ϑ. The distances from the top surface and the bottom surface of the kth layer to the referenced middle surface are represented by Z_{k+1} and Z_k accordingly. The partial cross-sectional view of the cylindrical shell is given in Fig. 5.2.

Consider the cylindrical shell in Fig. 5.1 and its cylindrical coordinate system. The coordinates, characteristics of the Lamé parameters and radii of curvatures are:

$$\alpha = x, \quad \beta = \theta, \quad A = 1, \quad B = R, \quad R_\alpha = \infty, \quad R_\beta = R \tag{5.1}$$

The above geometry parameters can be directly applied to the general shell equations derived in Chap. 1 to obtain those of cylindrical shells.

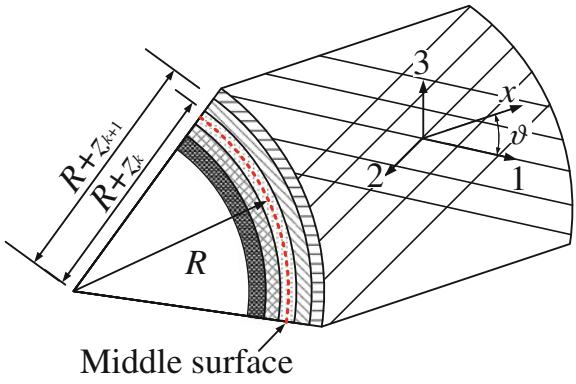

Fig. 5.2 Partial cross-sectional view of laminated circular cylindrical shells

5.1 Fundamental Equations of Thin Laminated Cylindrical Shells

We first derive the fundamental equations for thin laminated cylindrical shells (neglecting shear deformation and rotary inertia), followed by the thick ones. We will only consider laminated composite layers with cylindrical orthotropy. The equations are formulated for the general dynamic analysis of laminated cylindrical open shells. It can be readily applied to static (i.e., letting frequency ω equal to zero) and free vibration (i.e., neglecting the external load) analysis.

5.1.1 Kinematic Relations

Substituting Eq. (5.1) into Eq. (1.7), the middle surface strains and curvature changes of thin cylindrical shells can be specialized from those of general shells. They are formed in terms of middle surface displacements as:

$$\begin{aligned} \varepsilon_x^0 &= \frac{\partial u}{\partial x} & \chi_x &= -\frac{\partial^2 w}{\partial x^2} \\ \varepsilon_\theta^0 &= \frac{\partial v}{R\partial\theta} + \frac{w}{R} & \chi_\theta &= \frac{\partial v}{R^2\partial\theta} - \frac{\partial^2 w}{R^2\partial\theta^2} \\ \gamma_{x\theta}^0 &= \frac{\partial v}{\partial x} + \frac{\partial u}{R\partial\theta} & \chi_{x\theta} &= \frac{\partial v}{R\partial x} - 2\frac{\partial^2 w}{R\partial x\partial\theta} \end{aligned} \tag{5.2}$$

where ε_x^0, ε_θ^0 and $\gamma_{x\theta}^0$ denote the middle surface normal and shear strains. χ_x, χ_θ and $\chi_{x\theta}$ are the middle surface curvature and twist changes. Thus, the strain-displacement relations for an arbitrary point in the kth layer of a thin laminated cylindrical shell can be defined as:

$$\begin{aligned}\varepsilon_x &= \varepsilon_x^0 + z\chi_x \\ \varepsilon_\theta &= \varepsilon_\theta^0 + z\chi_\theta \\ \gamma_{x\theta} &= \gamma_{x\theta}^0 + z\chi_{x\theta}\end{aligned} \tag{5.3}$$

where $Z_{k+1} < z < Z_k$.

5.1.2 Stress-Strain Relations and Stress Resultants

The corresponding stress-strain relations in the kth layer can be obtained according to generalized Hooke's law as:

$$\begin{Bmatrix}\sigma_x \\ \sigma_\theta \\ \tau_{x\theta}\end{Bmatrix}_k = \begin{bmatrix}\overline{Q_{11}^k} & \overline{Q_{12}^k} & \overline{Q_{16}^k} \\ \overline{Q_{12}^k} & \overline{Q_{22}^k} & \overline{Q_{26}^k} \\ \overline{Q_{16}^k} & \overline{Q_{26}^k} & \overline{Q_{66}^k}\end{bmatrix} \begin{Bmatrix}\varepsilon_x \\ \varepsilon_\theta \\ \gamma_{x\theta}\end{Bmatrix}_k \tag{5.4}$$

where σ_x and σ_θ are the normal stresses in the x and θ directions, respectively. $\tau_{x\theta}$ is the corresponding shear stress. The lamina stiffness coefficients $\overline{Q_{ij}^k}\,(i,j = 1, 2, 6)$ represent the elastic properties of the material of the layer. They are written as in Eq. (1.12). Integrating the stresses over the thickness or substituting Eq. (5.1) into Eq. (1.14), the force and moment resultants of thin laminated cylindrical shells can be obtained in a matrix form as

$$\begin{bmatrix}N_x \\ N_\theta \\ N_{x\theta} \\ M_x \\ M_\theta \\ M_{x\theta}\end{bmatrix} = \begin{bmatrix}A_{11} & A_{12} & A_{16} & B_{11} & B_{12} & B_{16} \\ A_{12} & A_{22} & A_{26} & B_{12} & B_{22} & B_{26} \\ A_{16} & A_{26} & A_{66} & B_{16} & B_{26} & B_{66} \\ B_{11} & B_{12} & B_{16} & D_{11} & D_{12} & D_{16} \\ B_{12} & B_{22} & B_{26} & D_{12} & D_{22} & D_{26} \\ B_{16} & B_{26} & B_{66} & D_{16} & D_{26} & D_{66}\end{bmatrix} \begin{bmatrix}\varepsilon_x^0 \\ \varepsilon_\theta^0 \\ \gamma_{x\theta}^0 \\ \chi_x \\ \chi_\theta \\ \chi_{x\theta}\end{bmatrix} \tag{5.5}$$

where N_x, N_θ and $N_{x\theta}$ are the normal and shear force resultants and M_x, M_θ and $M_{x\theta}$ denote the bending and twisting moment resultants. The stiffness coefficient A_{ij}, B_{ij}, and D_{ij} are given in Eq. (1.15). It should be noted that for a laminated cylindrical shell which is symmetrically laminated with respect to the middle surface, the constants B_{ij} equal to zero.

5.1.3 Energy Functions

The strain energy function for thin laminated cylindrical shells during vibration can be written as:

$$U_s = \frac{1}{2}\int_x \int_\theta \left\{ \begin{array}{l} N_x\varepsilon_x^0 + N_\theta\varepsilon_\theta^0 + N_{x\theta}\gamma_{x\theta}^0 \\ +M_x\chi_x + M_\theta\chi_\theta + M_{x\theta}\chi_{x\theta} \end{array} \right\} Rd\theta dx \tag{5.6}$$

Substituting Eqs. (5.2) and (5.5) into Eq. (5.6), the strain energy function can be written in terms of middle surface displacements and divided to three components $U_s = U_{ss} + U_{sb} + U_{sbs}$, where U_{ss}, U_{sb} and U_{sbs} represent the stretching strain energy, bending strain energy and bending–stretching coupling energy, respectively.

$$U_{ss} = \frac{1}{2}\int_x \int_\theta \left\{ \begin{array}{l} A_{11}\left(\frac{\partial u}{\partial x}\right)^2 + \frac{A_{22}}{R^2}\left(\frac{\partial v}{\partial \theta} + w\right)^2 + A_{66}\left(\frac{\partial v}{\partial x} + \frac{\partial u}{R\partial \theta}\right)^2 \\ + \frac{2A_{12}}{R}\left(\frac{\partial v}{\partial \theta} + w\right)\left(\frac{\partial u}{\partial x}\right) + 2A_{16}\left(\frac{\partial v}{\partial x} + \frac{\partial u}{R\partial \theta}\right)\left(\frac{\partial u}{\partial x}\right) \\ + \frac{2A_{26}}{R}\left(\frac{\partial v}{\partial x} + \frac{\partial u}{R\partial \theta}\right)\left(\frac{\partial v}{\partial \theta} + w\right) \end{array} \right\} Rd\theta dx \tag{5.7a}$$

$$U_{sb} = \frac{1}{2}\int_x \int_\theta \left\{ \begin{array}{l} D_{11}\left(\frac{\partial^2 w}{\partial x^2}\right)^2 - \frac{2D_{12}}{R^2}\left(\frac{\partial v}{\partial \theta} - \frac{\partial^2 w}{\partial \theta^2}\right)\left(\frac{\partial^2 w}{\partial x^2}\right) - \frac{2D_{16}}{R} \\ \times\left(\frac{\partial^2 w}{\partial x^2}\right)\left(\frac{\partial v}{\partial x} - 2\frac{\partial^2 w}{\partial x \partial \theta}\right) + \frac{D_{22}}{R^4}\left(\frac{\partial v}{\partial \theta} - \frac{\partial^2 w}{\partial \theta^2}\right)^2 + \frac{D_{66}}{R^2} \\ \times\left(\frac{\partial v}{\partial x} - 2\frac{\partial^2 w}{\partial x \partial \theta}\right)^2 + \frac{2D_{26}}{R^3}\left(\frac{\partial v}{\partial x} - 2\frac{\partial^2 w}{\partial x \partial \theta}\right)\left(\frac{\partial v}{\partial \theta} - \frac{\partial^2 w}{\partial \theta^2}\right) \end{array} \right\} Rd\theta dx \tag{5.7b}$$

$$U_{sbs} = \int_x \int_\theta \left\{ \begin{array}{l} -B_{11}\left(\frac{\partial^2 w}{\partial x^2}\right)\left(\frac{\partial u}{\partial x}\right) + \frac{B_{12}}{R^2}\left(\frac{\partial v}{\partial \theta} - \frac{\partial^2 w}{\partial \theta^2}\right)\left(\frac{\partial u}{\partial x}\right) + \frac{B_{16}}{R} \\ \times\left(\frac{\partial v}{\partial x} - 2\frac{\partial^2 w}{\partial x \partial \theta}\right)\left(\frac{\partial u}{\partial x}\right) - \frac{B_{12}}{R}\left(\frac{\partial^2 w}{\partial x^2}\right)\left(\frac{\partial v}{\partial \theta} + w\right) + \frac{B_{22}}{R^3} \\ \times\left(\frac{\partial v}{\partial \theta} - \frac{\partial^2 w}{\partial \theta^2}\right)\left(\frac{\partial v}{\partial \theta} + w\right) + \frac{B_{26}}{R^2}\left(\frac{\partial v}{\partial x} - 2\frac{\partial^2 w}{\partial x \partial \theta}\right) \\ \times\left(\frac{\partial v}{\partial \theta} + w\right) - B_{16}\left(\frac{\partial^2 w}{\partial x^2}\right)\left(\frac{\partial v}{\partial x} + \frac{\partial u}{R\partial \theta}\right) + \frac{B_{26}}{R^2} \\ \times\left(\frac{\partial v}{\partial \theta} - \frac{\partial^2 w}{\partial \theta^2}\right)\left(\frac{\partial v}{\partial x} + \frac{\partial u}{R\partial \theta}\right) \\ + \frac{B_{66}}{R}\left(\frac{\partial v}{\partial x} + \frac{\partial u}{R\partial x}\right)\left(\frac{\partial v}{\partial x} - 2\frac{\partial^2 w}{\partial x \partial \theta}\right) \end{array} \right\} Rd\theta dx \tag{5.7c}$$

The corresponding kinetic energy (T) of the shells can be written as:

$$T = \frac{1}{2}\int_x \int_\theta I_0\left\{\left(\frac{\partial u}{\partial t}\right)^2 + \left(\frac{\partial v}{\partial t}\right)^2 + \left(\frac{\partial w}{\partial t}\right)^2\right\} Rd\theta dx \tag{5.8}$$

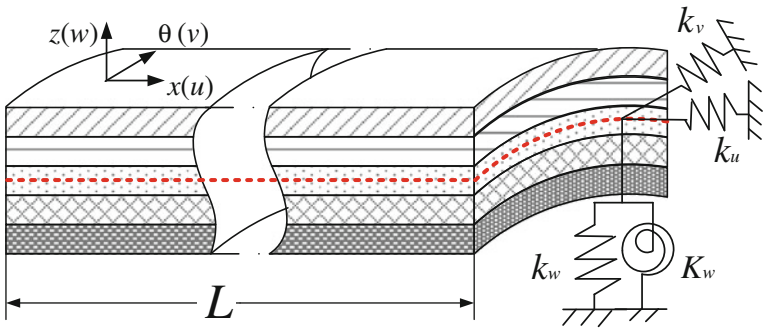

Fig. 5.3 Boundary conditions of thin laminated cylindrical shells

The inertia term I_0 is the same as in Eq. (1.19). Suppose q_x, q_θ and q_z are the external loads in the x, θ and z directions, respectively. Thus, the external work can be expressed as:

$$W_e = \int_x \int_\theta \{q_x u + q_\theta v + q_z w\} R d\theta dx \tag{5.9}$$

The same as usual, the general boundary conditions of a cylindrical shell are implemented by using the artificial spring boundary technique (see Sect. 1.2.3). Letting symbols $k_\psi^u, k_\psi^v, k_\psi^w$ and k_ψ^w ($\psi = x0$, $\theta 0$, $x1$ and $\theta 1$) to indicate the stiffness of the boundary springs at the boundaries $x = 0$, $\theta = 0$, $x = L$ and $\theta = \theta_0$, respectively (see Fig. 5.3). Therefore, the deformation strain energy stored in the boundary springs (U_{sp}) during vibration can be defined as:

$$\begin{aligned} U_{sp} = & \frac{1}{2}\int_\theta \left\{ \begin{array}{l} \left[k_{x0}^u u^2 + k_{x0}^v v^2 + k_{x0}^w w^2 + K_{x0}^w (\partial w/\partial x)\right]|_{x=0} \\ + \left[k_{x1}^u u^2 + k_{x1}^v v^2 + k_{x1}^w w^2 + K_{x1}^w (\partial w/\partial x)\right]|_{x=L} \end{array} \right\} R d\theta \\ & + \frac{1}{2}\int_x \left\{ \begin{array}{l} \left[k_{\theta 0}^u u^2 + k_{\theta 0}^v v^2 + k_{\theta 0}^w w^2 + K_{\theta 0}^w (\partial w/R\partial\theta)\right]|_{\theta=0} \\ + \left[k_{\theta 1}^u u^2 + k_{\theta 1}^v v^2 + k_{\theta 1}^w w^2 + K_{\theta 1}^w (\partial w/R\partial\theta)\right]|_{\theta=\theta_0} \end{array} \right\} dx \end{aligned} \tag{5.10}$$

5.1.4 Governing Equations and Boundary Conditions

The governing equations and boundary conditions of thin laminated cylindrical shells can be obtained by specializing form the governing equations of thin general laminated shells or applying the Hamilton's principle in the same manner as described in Sect. 1.2.4. Substituting Eq. (5.1) into Eq. (1.28) and then simplifying the expressions. Thus, the governing equations of thin laminated cylindrical shells become:

$$\begin{aligned}
&\frac{\partial N_x}{\partial x}+\frac{\partial N_{x\theta}}{R\partial\theta}+q_x=I_0\frac{\partial^2 u}{\partial t^2}\\
&\frac{\partial N_{x\theta}}{\partial x}+\frac{\partial N_\theta}{R\partial\theta}+\frac{Q_\theta}{R}+q_\theta=I_0\frac{\partial^2 v}{\partial t^2}\\
&-\frac{N_\theta}{R}+\frac{\partial Q_x}{\partial x}+\frac{\partial Q_\theta}{R\partial\theta}+q_z=I_0\frac{\partial^2 w}{\partial t^2}
\end{aligned} \tag{5.11}$$

where Q_x and Q_θ are defined as

$$\begin{aligned}
Q_x&=\frac{\partial M_x}{\partial x}+\frac{\partial M_{x\theta}}{R\partial\theta}\\
Q_\theta&=\frac{\partial M_{x\theta}}{\partial x}+\frac{\partial M_\theta}{R\partial\theta}
\end{aligned} \tag{5.12}$$

Substituting Eqs. (5.2), (5.5) and (5.13) into Eq. (5.12), the governing equations can be written in terms of middle surface displacements. These equations are proved useful when exact solutions are desired. These equations can be written as:

$$\left(\begin{bmatrix} L_{11} & L_{12} & L_{13}\\ L_{21} & L_{22} & L_{23}\\ L_{31} & L_{32} & L_{33}\end{bmatrix}-\omega^2\begin{bmatrix} -I_0 & 0 & 0\\ 0 & -I_0 & 0\\ 0 & 0 & -I_0\end{bmatrix}\right)\begin{bmatrix} u\\ v\\ w\end{bmatrix}=\begin{bmatrix} -p_x\\ -p_\theta\\ -p_z\end{bmatrix} \tag{5.13}$$

The coefficients of the linear operator L_{ij} are written as

$$\begin{aligned}
L_{11}&=A_{11}\frac{\partial^2}{\partial x^2}+\frac{2A_{16}}{R}\frac{\partial^2}{\partial x\partial\theta}+\frac{A_{66}}{R^2}\frac{\partial^2}{\partial\theta^2}\\
L_{12}&=\left(A_{16}+\frac{B_{16}}{R}\right)\frac{\partial^2}{\partial x^2}+\left(\frac{A_{12}}{R}+\frac{A_{66}}{R}+\frac{B_{12}+B_{66}}{R^2}\right)\frac{\partial^2}{\partial x\partial\theta}\\
&\quad+\left(\frac{A_{26}}{R^2}+\frac{B_{26}}{R^3}\right)\frac{\partial^2}{\partial\theta^2}=L_{21}\\
L_{13}&=-B_{11}\frac{\partial^3}{\partial x^3}-\frac{B_{26}}{R^3}\frac{\partial^3}{\partial\theta^3}-\frac{3B_{16}}{R}\frac{\partial^3}{\partial x^2\partial\theta}-\frac{B_{12}+2B_{66}}{R^2}\frac{\partial^3}{\partial x\partial\theta^2}\\
&\quad+\frac{A_{12}}{R}\frac{\partial}{\partial x}+\frac{A_{26}}{R^2}\frac{\partial}{\partial\theta}=-L_{31}\\
L_{22}&=\left(A_{66}+\frac{2B_{66}}{R}\right)\frac{\partial^2}{\partial x^2}+\left(\frac{2A_{26}}{R}+\frac{4B_{26}}{R^2}\right)\frac{\partial^2}{\partial x\partial\theta}+\left(\frac{A_{22}}{R^2}+\frac{2B_{22}}{R^3}\right)\frac{\partial^2}{\partial\theta^2}\\
L_{23}&=-\left(B_{16}+\frac{D_{16}}{R}\right)\frac{\partial^3}{\partial x^3}-\left(\frac{B_{22}}{R^3}+\frac{D_{22}}{R^4}\right)\frac{\partial^3}{\partial\theta^3}-3\left(\frac{B_{26}}{R^2}+\frac{D_{26}}{R^3}\right)\frac{\partial^3}{\partial x\partial\theta^2}\\
&\quad-\left(\frac{B_{12}+2B_{66}}{R}+\frac{D_{12}+2D_{66}}{R^2}\right)\frac{\partial^3}{\partial x^2\partial\theta}+\left(\frac{A_{26}}{R}+\frac{B_{26}}{R^2}\right)\frac{\partial}{\partial x}\\
&\quad+\left(\frac{A_{22}}{R^2}+\frac{B_{22}}{R^3}\right)\frac{\partial}{\partial\theta}=-L_{32}
\end{aligned} \tag{5.14}$$

$$L_{33} = 2\left(\frac{B_{12}}{R}\frac{\partial^2}{\partial x^2} + \frac{2B_{26}}{R^2}\frac{\partial^2}{\partial x \partial \theta} + \frac{B_{22}}{R^3}\frac{\partial^2}{\partial \theta^2}\right) - \frac{A_{22}}{R^2} - \frac{4D_{16}}{R}\frac{\partial^4}{\partial x^3 \partial \theta} - D_{11}\frac{\partial^4}{\partial x^4} - 2\left(\frac{D_{12}+2D_{66}}{R^2}\right)\frac{\partial^4}{\partial x^2 \partial \theta^2} - \frac{4D_{26}}{R^3}\frac{\partial^4}{\partial x \partial \theta^3} - \frac{D_{22}}{R^4}\frac{\partial^4}{\partial \theta^4}$$

And the general boundary conditions of thin laminated cylindrical shells are:

$$\begin{aligned}
x = 0: &\begin{cases} N_x - k_{x0}^u u = 0 \\ N_{x\theta} + \frac{M_{x\theta}}{R} - k_{x0}^v v = 0 \\ Q_x + \frac{\partial M_{x\theta}}{R\partial \theta} - k_{x0}^w w = 0 \\ -M_x - K_{x0}^w \frac{\partial w}{\partial x} = 0 \end{cases} \quad
x = L: \begin{cases} N_x + k_{x1}^u u = 0 \\ N_{x\theta} + \frac{M_{x\theta}}{R} + k_{x1}^v v = 0 \\ Q_x + \frac{\partial M_{x\theta}}{R\partial \theta} + k_{x1}^w w = 0 \\ -M_x + K_{x1}^w \frac{\partial w}{\partial x} = 0 \end{cases} \\
\theta = 0: &\begin{cases} N_{x\theta} - k_{\theta 0}^u u = 0 \\ N_\theta + \frac{M_\theta}{R} - k_{\theta 0}^v v = 0 \\ Q_\theta + \frac{\partial M_{x\theta}}{\partial x} - k_{\theta 0}^w w = 0 \\ -M_\theta - K_{\theta 0}^w \frac{\partial w}{R\partial \theta} = 0 \end{cases} \quad
\theta = \theta_0: \begin{cases} N_{x\theta} + k_{\theta 1}^u u = 0 \\ N_\theta + \frac{M_\theta}{R} + k_{\theta 1}^v v = 0 \\ Q_\theta + \frac{\partial M_{x\theta}}{\partial x} + k_{\theta 1}^w w = 0 \\ -M_\theta + K_{\theta 1}^w \frac{\partial w}{R\partial \theta} = 0 \end{cases}
\end{aligned} \tag{5.15}$$

The classification of the classical boundary conditions shown in Table 1.3 for thin laminated general shells is applicable for thin laminated cylindrical shells. Taking boundaries x = constant for example, the possible combinations for each classical boundary conditions are given in Table 5.1. Similar boundary conditions can be obtained for boundaries θ = constant.

It is obvious that there exists a huge number of possible combinations of boundary conditions for a thin laminated cylindrical shell. In contrast to most existing solution procedures, the artificial spring boundary technique offers a unified operation for laminated cylindrical shells with general boundary conditions. The stiffness of the boundary springs can take any value from zero to infinity to better model many real-world restraint conditions. Taking edge x = 0 for example, the widely encountered classical boundary conditions, such as F (completely free), S (simply-supported), SD (shear-diaphragm) and C (completely clamped) boundaries can be readily realized by assigning the stiffness of the boundary springs as:

$$\begin{aligned}
\text{F: } & k_{x0}^u = k_{x0}^v = k_{x0}^w = K_{x0}^w = 0 \\
\text{SD: } & k_{x0}^v = k_{x0}^w = 10^7 D, k_{x0}^u = K_{x0}^w = 0 \\
\text{S: } & k_{x0}^u = k_{x0}^v = k_{x0}^w = 10^7 D, K_{x0}^w = 0 \\
\text{C: } & k_{x0}^u = k_{x0}^v = k_{x0}^w = K_{x0}^w = 10^7 D
\end{aligned} \tag{5.16}$$

where $D = E_1 h^3/12(1 - \mu_{12}\,\mu_{21})$ is the flexural stiffness of the cylindrical shell.

Table 5.1 Possible classical boundary conditions for thin laminated cylindrical shells at boundaries x = constant

Boundary type	Conditions
Free boundary conditions	
F	$N_x = N_{x\theta} + \frac{M_{x\theta}}{R} = Q_x + \frac{\partial M_{x\theta}}{R\partial\theta} = M_x = 0$
F2	$u = N_{x\theta} + \frac{M_{x\theta}}{R} = Q_x + \frac{\partial M_{x\theta}}{R\partial\theta} = M_x = 0$
F3	$N_x = v = Q_x + \frac{\partial M_{x\theta}}{R\partial\theta} = M_x = 0$
F4	$u = v = Q_x + \frac{\partial M_{x\theta}}{R\partial\theta} = M_x = 0$
Simply supported boundary conditions	
S	$u = v = w = M_x = 0$
SD	$N_x = v = w = M_x = 0$
S3	$u = N_{x\theta} + \frac{M_{x\theta}}{R} = w = M_x = 0$
S4	$N_x = N_{x\theta} + \frac{M_{x\theta}}{R} = w = M_x = 0$
Clamped boundary conditions	
C	$u = v = w = \frac{\partial w}{\partial x} = 0$
C2	$N_x = v = w = \frac{\partial w}{\partial x} = 0$
C3	$u = N_{x\theta} + \frac{M_{x\theta}}{R} = w = \frac{\partial w}{\partial x} = 0$
C4	$N_x = N_{x\theta} + \frac{M_{x\theta}}{R} = w = \frac{\partial w}{\partial x} = 0$

5.2 Fundamental Equations of Thick Laminated Cylindrical Shells

The fundamental equations of thin laminated cylindrical shells presented in previous section are applicable only when the total thickness of the shell is smaller than 1/20 of the smallest of the wave lengths and/or radii of curvature (Qatu 2004) due to the fact that both shear deformation and rotary inertia are neglected in the formulation. This section presents fundamental equations of thick laminated cylindrical shells considering the effects of shear deformation and rotary inertia. The treatment that follows is a specialization of the general first-order shear deformation shell theory (SDST) given in Sect. 1.3 to those of the thick laminated cylindrical shells.

5.2.1 Kinematic Relations

On the basis of the shell model given in Fig. 5.1 and the assumptions of SDST, the displacement field of thick laminated cylindrical shells is defined in terms of the displacements and rotation components of the middle surface as

$$\begin{aligned} U(x,\theta,z) &= u(x,\theta) + z\phi_x \\ V(x,\theta,z) &= v(x,\theta) + z\phi_\theta \\ W(x,\theta,z) &= w(x,\theta) \end{aligned} \tag{5.17}$$

where u, v and w are the middle surface displacements of the shell in the axial, circumferential and radial directions, respectively, and ϕ_x and ϕ_θ represent the rotations of

transverse normal respect to θ- and x-axes. Specializing Eqs. (1.33) and (1.34) to those of cylindrical shells, the normal and shear strains at any point of the shell space can be defined in terms of the middle surface strains and curvature changes as:

$$\begin{aligned}
\varepsilon_x &= \varepsilon_x^0 + z\chi_x \\
\varepsilon_\theta &= \frac{1}{(1+z/R)}\left(\varepsilon_\theta^0 + z\chi_\theta\right) \\
\gamma_{x\theta} &= \left(\gamma_{x\theta}^0 + z\chi_{x\theta}\right) + \frac{1}{(1+z/R)}\left(\gamma_{\theta x}^0 + z\chi_{\theta x}\right) \\
\gamma_{xz} &= \gamma_{xz}^0 \\
\gamma_{\theta z} &= \frac{\gamma_{\theta z}^0}{(1+z/R)}
\end{aligned} \tag{5.18}$$

where γ_{xz}^0 and $\gamma_{\theta z}^0$ represent the transverse shear strains. The middle surface strains and curvature changes are defined as:

$$\begin{aligned}
\varepsilon_x^0 &= \frac{\partial u}{\partial x}, & \chi_x &= \frac{\partial \phi_x}{\partial x} \\
\varepsilon_\theta^0 &= \frac{\partial v}{R\partial\theta} + \frac{w}{R}, & \chi_\theta &= \frac{\partial \phi_\theta}{R\partial\theta} \\
\gamma_{x\theta}^0 &= \frac{\partial v}{\partial x}, & \chi_{x\theta} &\frac{\partial \phi_\theta}{\partial x} \\
\gamma_{\theta x}^0 &= \frac{\partial u}{R\partial\theta}, & \chi_{\theta x} &= \frac{\partial \phi_x}{R\partial\theta} \\
\gamma_{xz}^0 &= \frac{\partial w}{\partial x} + \phi_x \\
\gamma_{\theta z}^0 &= \frac{\partial w}{R\partial\theta} - \frac{v}{R} + \phi_\theta
\end{aligned} \tag{5.19}$$

5.2.2 Stress-Strain Relations and Stress Resultants

According to Hooke's law, the corresponding stresses in the kth layer of a thick laminated cylindrical shell can be obtained as:

$$\begin{Bmatrix} \sigma_x \\ \sigma_\theta \\ \tau_{\theta z} \\ \tau_{xz} \\ \tau_{x\theta} \end{Bmatrix}_k = \begin{bmatrix} \overline{Q_{11}^k} & \overline{Q_{12}^k} & 0 & 0 & \overline{Q_{16}^k} \\ \overline{Q_{12}^k} & \overline{Q_{22}^k} & 0 & 0 & \overline{Q_{26}^k} \\ 0 & 0 & \overline{Q_{44}^k} & \overline{Q_{45}^k} & 0 \\ 0 & 0 & \overline{Q_{45}^k} & \overline{Q_{55}^k} & 0 \\ \overline{Q_{16}^k} & \overline{Q_{26}^k} & 0 & 0 & \overline{Q_{66}^k} \end{bmatrix} \begin{Bmatrix} \varepsilon_x \\ \varepsilon_\theta \\ \gamma_{\theta z} \\ \gamma_{xz} \\ \gamma_{x\theta} \end{Bmatrix}_k \tag{5.20}$$

where τ_{xz} and $\tau_{\theta z}$ are the corresponding shear stress components. $\overline{Q_{ij}^k}$ $(i, j = 1, 2, 4, 5, 6)$ are known as the transformation stiffness coefficients, which represent the elastic properties of the material of the layer. They are given in Eq. (1.39). By carrying the integration of stresses over the cross-section, the force and moment resultants can be obtained:

$$\begin{bmatrix} N_x \\ N_{x\theta} \\ Q_x \end{bmatrix} = \int_{-h/2}^{h/2} \begin{bmatrix} \sigma_x \\ \tau_{x\theta} \\ \tau_{xz} \end{bmatrix} \left(1+\tfrac{z}{R}\right) dz, \quad \begin{bmatrix} N_\theta \\ N_{\theta x} \\ Q_\theta \end{bmatrix} = \int_{-h/2}^{h/2} \begin{bmatrix} \sigma_\theta \\ \tau_{\theta x} \\ \tau_{\theta z} \end{bmatrix} dz$$
$$\begin{bmatrix} M_x \\ M_{x\theta} \end{bmatrix} = \int_{-h/2}^{h/2} \begin{bmatrix} \sigma_x \\ \tau_{x\theta} \end{bmatrix} \left(1+\tfrac{z}{R}\right) z dz, \quad \begin{bmatrix} M_\theta \\ M_{\theta x} \end{bmatrix} = \int_{-h/2}^{h/2} \begin{bmatrix} \sigma_\theta \\ \tau_{\theta x} \end{bmatrix} z dz \tag{5.21}$$

It should be stressed that although $\tau_{x\theta}$ equals to $\tau_{\theta x}$ from the symmetry of the stress tensor, it is obvious from Eq. (5.21) that the shear force resultants $N_{x\theta}$ and $N_{\theta x}$ are not equal. Similarly, the twisting moment resultants $M_{x\theta}$ and $M_{\theta x}$ are not equal too. Carrying out the integration over the thickness, from layer to layer, yields

$$\begin{bmatrix} N_x \\ N_\theta \\ N_{x\theta} \\ N_{\theta x} \\ M_x \\ M_\theta \\ M_{x\theta} \\ M_{\theta x} \end{bmatrix} = \begin{bmatrix} \overline{A_{11}} & \overline{\overline{A_{12}}} & \overline{A_{16}} & \overline{\overline{A_{16}}} & \overline{B_{11}} & \overline{\overline{B_{12}}} & \overline{B_{16}} & \overline{\overline{B_{16}}} \\ \overline{\overline{A_{12}}} & \overline{A_{22}} & \overline{\overline{A_{26}}} & \overline{A_{26}} & \overline{\overline{B_{12}}} & \overline{B_{22}} & \overline{\overline{B_{26}}} & \overline{B_{26}} \\ \overline{A_{16}} & \overline{\overline{A_{26}}} & \overline{A_{66}} & \overline{\overline{A_{66}}} & \overline{B_{16}} & \overline{\overline{B_{26}}} & \overline{B_{66}} & \overline{\overline{B_{66}}} \\ \overline{\overline{A_{16}}} & \overline{A_{26}} & \overline{\overline{A_{66}}} & \overline{A_{66}} & \overline{\overline{B_{16}}} & \overline{B_{26}} & \overline{\overline{B_{66}}} & \overline{B_{66}} \\ \overline{B_{11}} & \overline{\overline{B_{12}}} & \overline{B_{16}} & \overline{\overline{B_{16}}} & \overline{D_{11}} & \overline{\overline{D_{12}}} & \overline{D_{16}} & \overline{\overline{D_{16}}} \\ \overline{\overline{B_{12}}} & \overline{B_{22}} & \overline{\overline{B_{26}}} & \overline{B_{26}} & \overline{\overline{D_{12}}} & \overline{D_{22}} & \overline{\overline{D_{26}}} & \overline{D_{26}} \\ \overline{B_{16}} & \overline{\overline{B_{26}}} & \overline{B_{66}} & \overline{\overline{B_{66}}} & \overline{D_{16}} & \overline{\overline{D_{26}}} & \overline{D_{66}} & \overline{\overline{D_{66}}} \\ \overline{\overline{B_{16}}} & \overline{B_{26}} & \overline{\overline{B_{66}}} & \overline{B_{66}} & \overline{\overline{D_{16}}} & \overline{D_{26}} & \overline{\overline{D_{66}}} & \overline{D_{66}} \end{bmatrix} \begin{bmatrix} \varepsilon_x^0 \\ \varepsilon_\theta^0 \\ \gamma_{x\theta}^0 \\ \gamma_{\theta x}^0 \\ \chi_x \\ \chi_\theta \\ \chi_{x\theta} \\ \chi_{\theta x} \end{bmatrix} \tag{5.22}$$

$$\begin{bmatrix} Q_\theta \\ Q_x \end{bmatrix} = \begin{bmatrix} \overline{\overline{A_{44}}} & A_{45} \\ A_{45} & \overline{A_{55}} \end{bmatrix} \begin{bmatrix} \gamma_{\theta z}^0 \\ \gamma_{xz}^0 \end{bmatrix} \tag{5.23}$$

The stiffness coefficients A_{ij}, B_{ij} and D_{ij} are given as in Eq. (1.43). The stiffness coefficients $\overline{A_{ij}}, \overline{B_{ij}}, \overline{D_{ij}}, \overline{\overline{A_{ij}}}, \overline{\overline{B_{ij}}}$ and $\overline{\overline{D_{ij}}}$ are defined as:

$$\begin{aligned}
\overline{A_{ij}} &= A_{ij} + B_{ij}/R \\
\overline{B_{ij}} &= B_{ij} + D_{ij}/R \\
\overline{D_{ij}} &= D_{ij} + E_{ij}/R \\
\overline{\overline{A_{ij}}} &= R \sum_{k=1}^{N_L} \overline{Q_{ij}^k} \ln\left(\frac{R+z_{k+1}}{R+z_k}\right) \qquad (i,j = 1,2,6) \\
\overline{\overline{A_{ij}}} &= K_s R \sum_{k=1}^{N_L} \overline{Q_{ij}^k} \ln\left(\frac{R+z_{k+1}}{R+z_k}\right) \qquad (i,j = 4,5) \\
\overline{\overline{B_{ij}}} &= R \sum_{k=1}^{N_L} \overline{Q_{ij}^k} \left[(z_{k+1}-z_k) - R \ln\left(\frac{R+z_{k+1}}{R+z_k}\right)\right] \\
\overline{\overline{D_{ij}}} &= \sum_{k=1}^{N_L} \overline{Q_{ij}^k} \left[-R^2(z_{k+1}-z_k) + \frac{R}{2}\left(z_{k+1}^2 - z_k^2\right) + R^3 \ln\left(\frac{R+z_{k+1}}{R+z_k}\right)\right]
\end{aligned} \tag{5.24}$$

where K_s is the shear correction factor. N_L represents the mount of the layers. E_{ij} are defined as

$$E_{ij} = \frac{1}{4}\sum_{k=1}^{N_L} \overline{Q_{ij}^k}\left[z_{k+1}^4 - z_k^4\right], \quad (i,j = 1,2,6) \tag{5.25}$$

The above equations include the effects of the deepness term z/R, and thus create complexities in carrying out the integration and the follow-up programming. Figures 3.7 and 3.8 showed that the effects of the deepness term z/R on the frequency parameters of an extremely deep, unsymmetrically laminated curved beam ($\theta_0 = 286.48°$) with thickness-to-radius ratio $h/R = 0.1$ are very small and the maximum effect is less than 0.41 % for the worse case. These results can be used in establishing the limits of shell theories and shell equations as well. When the FSDT is applied to thin and moderately thick cylindrical shells, the deepness term z/R can be neglected (Qu et al. 2013a, b; Jin et al. 2013b, 2014a; Ye et al. 2014b), in such case, the force and moment resultants of cylindrical shells (Eq. (5.23)) can be rewritten as:

$$\begin{bmatrix} N_x \\ N_\theta \\ N_{x\theta} \\ N_{\theta x} \\ M_x \\ M_\theta \\ M_{x\theta} \\ M_{\theta x} \end{bmatrix} = \begin{bmatrix} A_{11} & A_{12} & A_{16} & A_{16} & B_{11} & B_{12} & B_{16} & B_{16} \\ A_{12} & A_{22} & A_{26} & A_{26} & B_{12} & B_{22} & B_{26} & B_{26} \\ A_{16} & A_{26} & A_{66} & A_{66} & B_{16} & B_{26} & B_{66} & B_{66} \\ A_{16} & A_{26} & A_{66} & A_{66} & B_{16} & B_{26} & B_{66} & B_{66} \\ B_{11} & B_{12} & B_{16} & B_{16} & D_{11} & D_{12} & D_{16} & D_{16} \\ B_{12} & B_{22} & B_{26} & B_{26} & D_{12} & D_{22} & D_{26} & D_{26} \\ B_{16} & B_{26} & B_{66} & B_{66} & D_{16} & D_{26} & D_{66} & D_{66} \\ B_{16} & B_{26} & B_{66} & B_{66} & D_{16} & D_{26} & D_{66} & D_{66} \end{bmatrix} \begin{bmatrix} \varepsilon_x^0 \\ \varepsilon_\theta^0 \\ \gamma_{x\theta}^0 \\ \gamma_{\theta x}^0 \\ \chi_x \\ \chi_\theta \\ \chi_{x\theta} \\ \chi_{\theta x} \end{bmatrix} \tag{5.26}$$

$$\begin{bmatrix} Q_\theta \\ Q_x \end{bmatrix} = \begin{bmatrix} A_{44} & A_{45} \\ A_{45} & A_{55} \end{bmatrix} \begin{bmatrix} \gamma_{\theta z}^0 \\ \gamma_{xz}^0 \end{bmatrix} \tag{5.27}$$

5.2.3 Energy Functions

The strain energy (U_s) of laminated cylindrical shells including shear deformation effects during vibration can be defined in terms of the middle surface strains and curvature changes and stress resultants as

$$U_s = \frac{1}{2}\int_x \int_\theta \left\{ \begin{matrix} N_x\varepsilon_x^0 + N_\theta\varepsilon_\theta^0 + N_{x\theta}\gamma_{x\theta}^0 + N_{\theta x}\gamma_{\theta x}^0 + M_x\chi_x \\ +M_\theta\chi_\theta + M_{x\theta}\chi_{x\theta} + M_{\theta x}\chi_{\theta x} + Q_\theta\gamma_{\theta z} + Q_x\gamma_{xz} \end{matrix} \right\} Rd\theta dx \tag{5.28}$$

Substituting Eqs. (5.19), (5.22) and (5.23) into Eq. (5.28), the strain energy of the shell can be expressed in terms of middle surface displacements (u, v, w) and rotation components (ϕ_x, ϕ_θ).

The kinetic energy (T) of the cylindrical shells including rotary inertia is written as:

$$T = \int_x \int_\theta \int_{-h/2}^{h/2} \frac{\rho^k}{2} \left\{ \left(\frac{\partial u}{\partial t} + z\frac{\partial \phi_x}{\partial t}\right)^2 + \left(\frac{\partial w}{\partial t}\right)^2 + \left(\frac{\partial v}{\partial t} + z\frac{\partial \phi_\theta}{\partial t}\right)^2 \right\} (R+z) dz d\theta dx$$

$$= \frac{1}{2} \int_x \int_\theta \left\{ \begin{array}{l} \overline{I_0}\left(\frac{\partial u}{\partial t}\right)^2 + 2\overline{I_1}\frac{\partial u}{\partial t}\frac{\partial \phi_x}{\partial t} + \overline{I_2}\left(\frac{\partial \phi_x}{\partial t}\right)^2 + \overline{I_0}\left(\frac{\partial v}{\partial t}\right)^2 \\ + 2\overline{I_1}\frac{\partial v}{\partial t}\frac{\partial \phi_\theta}{\partial t} + \overline{I_2}\left(\frac{\partial \phi_\theta}{\partial t}\right)^2 + \overline{I_0}\left(\frac{\partial w}{\partial t}\right)^2 \end{array} \right\} R d\theta dx \tag{5.29}$$

where the inertia terms are:

$$\begin{aligned} \overline{I_0} &= I_0 + I_1/R \\ \overline{I_1} &= I_1 + I_2/R \\ \overline{I_2} &= I_2 + I_3/R \\ [I_0, I_1, I_2, I_3] &= \sum_{k=1}^{N_L} \int_{z_k}^{z_{k+1}} \rho^k [1, z, z^2, z^3] dz \end{aligned} \tag{5.30}$$

in which ρ^k is the mass of the kth layer per unit middle surface area. Assuming the distributed external forces q_x, q_θ and q_z are in the x, θ and z directions, respectively, and m_x and m_θ represent the external couples in the middle surface, thus, the work done by the external forces and moments is

$$W_e = \int_x \int_\theta \{q_x u + q_\theta v + q_z w + m_x \phi_x + m_\theta \phi_\theta\} R d\theta dx \tag{5.31}$$

Using the artificial spring boundary technique as described earlier, let $k_\psi^u, k_\psi^u, k_\psi^w$, K_ψ^x, and $K_\psi^\theta (\psi = x0, \theta 0, x1 \text{ and } \theta 1)$ to represent the rigidities (per unit length) of the boundary springs at the boundaries $x = 0$, $\theta = 0$, $x = L$ and $\theta = \theta_0$, respectively. Therefore, the deformation strain energy (U_{sp}) stored in the boundary springs during vibration is defined as (Fig. 5.4):

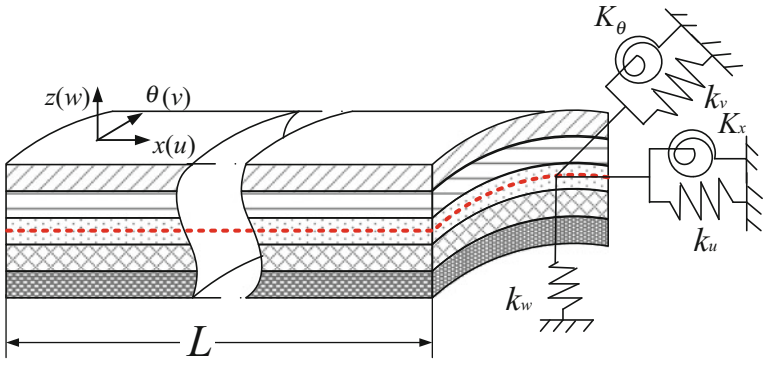

Fig. 5.4 Boundary conditions of thick laminated cylindrical shells

$$U_{sp} = \frac{1}{2}\int_{\theta}\left\{\begin{array}{l}\left[k_{x0}^{u}u^2 + k_{x0}^{v}v^2 + k_{x0}^{w}w^2 + K_{x0}^{x}\phi_x^2 + K_{x0}^{\theta}\phi_\theta^2\right]|_{x=0} \\ +\left[k_{x1}^{u}u^2 + k_{x1}^{v}v^2 + k_{x1}^{w}w^2 + K_{x1}^{x}\phi_x^2 + K_{x1}^{\theta}\phi_\theta^2\right]|_{x=L}\end{array}\right\}Rd\theta$$
$$+\frac{1}{2}\int_{x}\left\{\begin{array}{l}\left[k_{\theta0}^{u}u^2 + k_{\theta0}^{v}v^2 + k_{\theta0}^{w}w^2 + K_{\theta0}^{x}\phi_x^2 + K_{\theta0}^{\theta}\phi_\theta^2\right]|_{\theta=0} \\ +\left[k_{\theta1}^{u}u^2 + k_{\theta1}^{v}v^2 + k_{\theta1}^{w}w^2 + K_{\theta1}^{x}\phi_x^2 + K_{\theta1}^{\theta}\phi_\theta^2\right]|_{\theta=\theta_0}\end{array}\right\}dx \tag{5.32}$$

5.2.4 Governing Equations and Boundary Conditions

The governing equations and boundary conditions of thick laminated cylindrical shells can be obtained by substituting Eq. (5.1) into those of laminated general thick shells (Eq. (1.59)). According to Eq. (1.59), we have

$$\begin{aligned}
&\frac{\partial N_x}{\partial x} + \frac{\partial N_{\theta x}}{R\partial\theta} + q_x = \overline{I}_0\frac{\partial^2 u}{\partial t^2} + \overline{I}_1\frac{\partial^2 \phi_x}{\partial t^2}\\
&\frac{\partial N_{x\theta}}{\partial x} + \frac{\partial N_\theta}{R\partial\theta} + \frac{Q_\theta}{R} + q_\theta = \overline{I}_0\frac{\partial^2 v}{\partial t^2} + \overline{I}_1\frac{\partial^2 \phi_\theta}{\partial t^2}\\
&-\frac{N_\theta}{R} + \frac{\partial Q_x}{\partial x} + \frac{\partial Q_\theta}{R\partial\theta} + q_z = \overline{I}_0\frac{\partial^2 w}{\partial t^2}\\
&\frac{\partial M_x}{\partial x} + \frac{\partial M_{\theta x}}{R\partial\theta} - Q_x + m_x = \overline{I}_1\frac{\partial^2 u}{\partial t^2} + \overline{I}_2\frac{\partial^2 \phi_x}{\partial t^2}\\
&\frac{\partial M_{x\theta}}{\partial x} + \frac{\partial M_\beta}{R\partial\theta} - Q_\theta + m_\theta = \overline{I}_1\frac{\partial^2 v}{\partial t^2} + \overline{I}_2\frac{\partial^2 \phi_\theta}{\partial t^2}
\end{aligned} \tag{5.33}$$

Substituting Eqs. (5.19), (5.22) and (5.23) into above equations, the governing equations of thick cylindrical shells can be written in terms of displacements as

$$\left(\begin{bmatrix} L_{11} & L_{12} & L_{13} & L_{14} & L_{15}\\ L_{21} & L_{22} & L_{23} & L_{24} & L_{25}\\ L_{31} & L_{32} & L_{33} & L_{34} & L_{35}\\ L_{41} & L_{42} & L_{43} & L_{44} & L_{45}\\ L_{51} & L_{52} & L_{53} & L_{54} & L_{55}\end{bmatrix} - \omega^2\begin{bmatrix} M_{11} & 0 & 0 & M_{14} & 0\\ 0 & M_{22} & 0 & 0 & M_{25}\\ 0 & 0 & M_{33} & 0 & 0\\ M_{41} & 0 & 0 & M_{44} & 0\\ 0 & M_{52} & 0 & 0 & M_{55}\end{bmatrix}\right)\begin{bmatrix} u\\ v\\ w\\ \phi_x\\ \phi_\theta\end{bmatrix}$$
$$= \begin{bmatrix} -p_x\\ -p_y\\ -p_z\\ -m_x\\ -m_\theta\end{bmatrix} \tag{5.34}$$

The coefficients of the linear operator L_{ij} and M_{ij} are given as

$$
\begin{aligned}
L_{11} &= \overline{A_{11}}\frac{\partial^2}{\partial x^2} + \frac{2A_{16}}{R}\frac{\partial^2}{\partial x\partial\theta} + \frac{\overline{\overline{A_{66}}}}{R^2}\frac{\partial^2}{\partial\theta^2} \\
L_{12} &= L_{21} = \overline{A_{16}}\frac{\partial^2}{\partial x^2} + \left(\frac{A_{12}}{R} + \frac{A_{66}}{R}\right)\frac{\partial^2}{\partial x\partial\theta} + \frac{\overline{\overline{A_{26}}}}{R^2}\frac{\partial^2}{\partial\theta^2} \\
L_{13} &= -L_{31} = \frac{A_{12}}{R}\frac{\partial}{\partial x} + \frac{\overline{\overline{A_{26}}}}{R^2}\frac{\partial}{\partial\theta} \\
L_{14} &= L_{41} = \overline{B_{11}}\frac{\partial^2}{\partial x^2} + \frac{2B_{16}}{R}\frac{\partial^2}{\partial x\partial\theta} + \frac{\overline{\overline{B_{66}}}}{R^2}\frac{\partial^2}{\partial\theta^2} \\
L_{15} &= L_{51} = \overline{B_{16}}\frac{\partial^2}{\partial x^2} + \left(\frac{B_{12}}{R} + \frac{B_{66}}{R}\right)\frac{\partial^2}{\partial x\partial\theta} + \frac{\overline{\overline{B_{26}}}}{R^2}\frac{\partial^2}{\partial\theta^2} \\
L_{22} &= \overline{A_{66}}\frac{\partial^2}{\partial x^2} + \frac{2A_{26}}{R}\frac{\partial^2}{\partial x\partial\theta} + \frac{\overline{\overline{A_{22}}}}{R^2}\frac{\partial^2}{\partial\theta^2} - \frac{\overline{\overline{A_{44}}}}{R^2} \\
L_{23} &= -L_{32} = \left(\frac{A_{26} + A_{45}}{R}\right)\frac{\partial}{\partial x} + \left(\frac{\overline{\overline{A_{22}}} + \overline{\overline{A_{44}}}}{R^2}\right)\frac{\partial}{\partial\theta} \\
L_{24} &= L_{42} = \overline{B_{16}}\frac{\partial^2}{\partial x^2} + (\frac{B_{12} + B_{66}}{R})\frac{\partial^2}{\partial x\partial\theta} + \frac{\overline{\overline{B_{26}}}}{R^2}\frac{\partial^2}{\partial\theta^2} + \frac{A_{45}}{R} \\
L_{25} &= L_{52} = \overline{B_{66}}\frac{\partial^2}{\partial x^2} + \frac{2B_{26}}{R}\frac{\partial^2}{\partial x\partial\theta} + \frac{\overline{\overline{B_{22}}}}{R^2}\frac{\partial^2}{\partial\theta^2} + \frac{\overline{\overline{A_{44}}}}{R^2} \\
L_{33} &= \overline{A_{55}}\frac{\partial^2}{\partial x^2} + \frac{2A_{45}}{R}\frac{\partial^2}{\partial x\partial\theta} + \frac{\overline{\overline{A_{44}}}}{R^2}\frac{\partial^2}{\partial\theta^2} - \frac{\overline{\overline{A_{22}}}}{R^2} \\
L_{34} &= -L_{43} = (\overline{A_{55}} - \frac{B_{12}}{R})\frac{\partial}{\partial x} + (\frac{A_{45}}{R} - \frac{\overline{\overline{B_{26}}}}{R^2})\frac{\partial}{\partial\theta} \\
L_{35} &= -L_{53} = (A_{45} - \frac{B_{26}}{R})\frac{\partial}{\partial x} + (\frac{\overline{\overline{A_{44}}}}{R} - \frac{\overline{\overline{B_{22}}}}{R^2})\frac{\partial}{\partial\theta} \\
L_{44} &= \overline{D_{11}}\frac{\partial^2}{\partial x^2} + \frac{2D_{16}}{R}\frac{\partial^2}{\partial x\partial\theta} + \frac{\overline{\overline{D_{66}}}}{R^2}\frac{\partial^2}{\partial\theta^2} - \overline{A_{55}} \\
L_{45} &= L_{54} = \overline{D_{16}}\frac{\partial^2}{\partial x^2} + \left(\frac{D_{12}}{R} + \frac{D_{66}}{R}\right)\frac{\partial^2}{\partial x\partial\theta} + \frac{\overline{\overline{D_{26}}}}{R^2}\frac{\partial^2}{\partial\theta^2} - A_{45} \\
L_{55} &= \overline{D_{66}}\frac{\partial^2}{\partial x^2} + \frac{2D_{26}}{R}\frac{\partial^2}{\partial x\partial\theta} + \frac{\overline{\overline{D_{22}}}}{R^2}\frac{\partial^2}{\partial\theta^2} - \overline{\overline{A_{44}}} \\
M_{11} &= M_{22} = M_{33} = -\overline{I_0} \\
M_{14} &= M_{41} = M_{15} = M_{51} = -\overline{I_1} \\
M_{44} &= M_{55} = -\overline{I_2}
\end{aligned}
\tag{5.35}
$$

According to Eqs. (1.60) and (1.61), the general boundary conditions of thick laminated cylindrical shells are

$$
\begin{aligned}
x=0:&\begin{cases} N_x-k_{x0}^{u}u=0\\ N_{x\theta}-k_{x0}^{v}v=0\\ Q_x-k_{x0}^{w}w=0\\ M_x-K_{x0}^{x}\phi_x=0\\ M_{x\theta}-K_{x0}^{\theta}\phi_\theta=0 \end{cases}
\qquad
x=L:\begin{cases} N_x+k_{x1}^{u}u=0\\ N_{x\theta}+k_{x1}^{v}v=0\\ Q_x+k_{x1}^{w}w=0\\ M_x+K_{x1}^{x}\phi_x=0\\ M_{x\theta}+K_{x1}^{\theta}\phi_\theta=0 \end{cases}\\
\theta=0:&\begin{cases} N_{\theta x}-k_{\theta 0}^{u}u=0\\ N_{\theta}-k_{\theta 0}^{v}v=0\\ Q_{\theta}-k_{\theta 0}^{w}w=0\\ M_{\theta x}-K_{\theta 0}^{x}\phi_x=0\\ M_{\theta}-K_{\theta 0}^{\theta}\phi_\theta=0 \end{cases}
\qquad
\theta=\theta_0:\begin{cases} N_{\theta x}+k_{\theta 1}^{u}u=0\\ N_{\theta}+k_{\theta 1}^{v}v=0\\ Q_{\theta}+k_{\theta 1}^{w}w=0\\ M_{\theta x}+K_{\theta 1}^{x}\phi_x=0\\ M_{\theta}+K_{\theta 1}^{\theta}\phi_\theta=0 \end{cases}
\end{aligned}
\tag{5.36}
$$

Thick cylindrical shells can have 24 possible classical boundary conditions at each edge. This yields a numerous combinations of boundary conditions, particular for open cylindrical shells. Table 5.2 shows the 24 possible classical boundary conditions for boundaries x = constant, similar boundary conditions can be obtained for boundaries θ = constant (only existing in open cylindrical shells).

Classical boundary conditions can be seen as special cases of the elastic ones. By using the artificial spring boundary technique, all the aforementioned classical boundary conditions can be readily generated by assigning the boundary springs at proper stiffness. Although we can obtain accurate solutions for laminated cylindrical shells with arbitrary classical conditions and their combinations, in this chapter we will consider four typical boundary conditions that are frequently encountered in practices, namely, F, SD, S and C boundary conditions. Taking edge $x = 0$ for example, the corresponding spring stiffness for the four classical boundary conditions are given below (N/m and N/rad are utilized as the units of the stiffness about the translational springs and rotational springs, respectively):

$$
\begin{aligned}
\text{F: } & k_{x0}^{u}=k_{x0}^{v}=k_{x0}^{w}=K_{x0}^{x}=K_{x0}^{\theta}=0\\
\text{SD: } & k_{x0}^{v}=k_{x0}^{w}=K_{x0}^{\theta}=10^7D,\quad k_{x0}^{u}=K_{x0}^{x}=0\\
\text{S: } & k_{x0}^{u}=k_{x0}^{v}=k_{x0}^{w}=K_{x0}^{\theta}=10^7D,\quad K_{x0}^{x}=0\\
\text{C: } & k_{x0}^{u}=k_{x0}^{v}=k_{x0}^{w}=K_{x0}^{x}=K_{x0}^{\theta}=10^7D
\end{aligned}
\tag{5.37}
$$

5.3 Vibration of Laminated Closed Cylindrical Shells

Thin and thick laminated closed cylindrical shells with different boundary conditions, lamination schemes and geometry parameters are treated in the subsequent analysis. Both solutions in the framework of the CST and SDST (neglecting the

Table 5.2 Possible classical boundary conditions for thick cylindrical shells at each boundary of x = constant

Boundary type	Conditions
Free boundary conditions	
F	$N_x = N_{x\theta} = Q_x = M_x = M_{x\theta} = 0$
F2	$u = N_{x\theta} = Q_x = M_x = M_{x\theta} = 0$
F3	$N_x = v = Q_x = M_x = M_{x\theta} = 0$
F4	$u = v = Q_x = M_x = M_{x\theta} = 0$
F5	$N_x = N_{x\theta} = Q_x = M_x = \phi_\theta = 0$
F6	$u = N_{x\theta} = Q_x = M_x = \phi_\theta = 0$
F7	$N_x = v = Q_x = M_x = \phi_\theta = 0$
F8	$u = v = Q_x = M_x = \phi_\theta = 0$
Simply supported boundary conditions	
S	$u = v = w = M_x = \phi_\theta = 0$
SD	$N_x = v = w = M_x = \phi_\theta = 0$
S3	$u = N_{x\theta} = w = M_x = \phi_\theta = 0$
S4	$N_x = N_{x\theta} = w = M_x = \phi_\theta = 0$
S5	$u = v = w = M_x = M_{x\theta} = 0$
S6	$N_x = v = w = M_x = M_{x\theta} = 0$
S7	$u = N_{x\theta} = w = M_x = M_{x\theta} = 0$
S8	$N_x = N_{x\theta} = w = M_x = M_{x\theta} = 0$
Clamped boundary conditions	
C	$u = v = w = \phi_x = \phi_\theta = 0$
C2	$N_x = v = w = \phi_x = \phi_\theta = 0$
C3	$u = N_{x\theta} = w = \phi_x = \phi_\theta = 0$
C4	$N_x = N_{x\theta} = w = \phi_x = \phi_\theta = 0$
C5	$u = v = w = \phi_x = M_{x\theta} = 0$
C6	$N_x = v = w = \phi_x = M_{x\theta} = 0$
C7	$u = N_{x\theta} = w = \phi_x = M_{x\theta} = 0$
C8	$N_x = N_{x\theta} = w = \phi_x = M_{x\theta} = 0$

deepness term z/R, i.e., Eq. (5.26)) are presented. Natural frequencies and mode shapes of the cylindrical shells are obtained by applying the previous developed modified Fourier series and weak form solution procedure. For a laminated closed cylindrical shell, there exist two boundaries, i.e., $x = 0$ and $x = L$. For the sake of simplicity, a two-letter string is employed to represent the boundary condition of a cylindrical shell, such as F–C indicates the shell with edges $x = 0$ and $x = L$ having F and C boundary conditions, respectively. Unless otherwise stated, the natural frequencies of the considered shells are expressed in the non-dimensional parameters as $\Omega = (\omega L^2/h)\sqrt{\rho/E_2}$ and the material properties of the layers of laminated cylindrical shells under consideration are given as: E_2 = 10 GPa, E_1/E_2 = open, $\mu_{12} = 0.25$, $G_{12} = 0.6\ E_2$, $G_{13} = G_{23} = 0.5\ E_2$, ρ = 1,450 kg/m^3.

Considering the circumferential symmetry of closed circular cylindrical shells, the assumed 2D displacement field can be reduced to a quasi 1D problem through Fourier decomposition of the circumferential wave motion. Thus, taking the FSDT displacement field for example, each displacement and rotation component of a closed circular cylindrical shell is expanded as the following form:

$$\begin{aligned}
u(x,\theta) &= \sum_{m=0}^{M}\sum_{n=0}^{N} A_{mn}\cos\lambda_m x\cos n\theta + \sum_{l=1}^{2}\sum_{n=0}^{N} a_{\ln}P_l(x)\cos n\theta \\
v(x,\theta) &= \sum_{m=0}^{M}\sum_{n=0}^{N} B_{mn}\cos\lambda_m x\sin n\theta + \sum_{l=1}^{2}\sum_{n=0}^{N} b_{\ln}P_l(x)\sin n\theta \\
w(x,\theta) &= \sum_{m=0}^{M}\sum_{n=0}^{N} C_{mn}\cos\lambda_m x\cos n\theta + \sum_{l=1}^{2}\sum_{n=0}^{N} c_{\ln}P_l(x)\cos n\theta \\
\phi_x(x,\theta) &= \sum_{m=0}^{M}\sum_{n=0}^{N} D_{mn}\cos\lambda_m x\cos n\theta + \sum_{l=1}^{2}\sum_{n=0}^{N} d_{\ln}P_l(x)\cos n\theta \\
\phi_\theta(x,\theta) &= \sum_{m=0}^{M}\sum_{n=0}^{N} E_{mn}\cos\lambda_m x\sin n\theta + \sum_{l=1}^{2}\sum_{n=0}^{N} e_{\ln}P_l(x)\sin n\theta
\end{aligned} \tag{5.38}$$

where $\lambda_m = m\pi/L$. n represents the circumferential wave number of the corresponding mode. It should be note that n is a non-negative integer. Interchanging of $\sin n\theta$ and $\cos n\theta$ in Eq. (5.38), another set of free vibration modes (anti-symmetric modes) can be obtained. A_{mn}, B_{mn}, C_{mn}, D_{mn} and E_{mn} are expansion coefficients of standard cosine Fourier series. a_{ln}, b_{ln}, c_{ln}, d_{ln} and e_{ln} are the corresponding supplement coefficients. M and N denote the truncation numbers with respect to variables x and θ, respectively. According to Eq. (5.35), it is obvious that each displacement and rotation component in the FSDT displacement field is required to have up to the second derivatives. Therefore, two auxiliary polynomial functions $P_l(x)$ are introduced in each displacement expression to remove all the discontinuities potentially associated with the first-order derivatives at the boundaries. These auxiliary functions are defined as (Ye et al. 2014a, d, e)

$$P_1(x) = x\left(\frac{x}{L}-1\right)^2 \quad P_2(x) = \frac{x^2}{L}\left(\frac{x}{L}-1\right) \tag{5.39}$$

According to Eq. (5.14), it can be seen that the displacements in the CST displacement field are required to have up to the third (u and v) or fourth (w) derivatives. In such case, the axial, circumferential and radial displacements of a closed circular cylindrical shell are expanded as a 1-D modified Fourier series in which four auxiliary polynomial functions should be introduced to remove all the discontinuities potentially associated with the first-order and third-order derivatives at the boundaries:

$$
\begin{aligned}
u(x,\theta) &= \sum_{m=0}^{M}\sum_{n=0}^{N} A_{mn}\cos\lambda_m x\cos n\theta + \sum_{l=1}^{4}\sum_{n=0}^{N} a_{\ln} P_l(x)\cos n\theta \\
v(x,\theta) &= \sum_{m=0}^{M}\sum_{n=0}^{N} B_{mn}\cos\lambda_m x\sin n\theta + \sum_{l=1}^{4}\sum_{n=0}^{N} b_{\ln} P_l(x)\sin n\theta \\
w(x,\theta) &= \sum_{m=0}^{M}\sum_{n=0}^{N} C_{mn}\cos\lambda_m x\cos n\theta + \sum_{l=1}^{4}\sum_{n=0}^{N} c_{\ln} P_l(x)\cos n\theta
\end{aligned}
\tag{5.40}
$$

where the four auxiliary polynomial functions P_l (x) are given as (Zhang and Li 2009)

$$
\begin{aligned}
P_1(x) &= \frac{9L}{4\pi}\sin(\frac{\pi x}{2L}) - \frac{L}{12\pi}\sin(\frac{3\pi x}{2L}) \\
P_2(x) &= -\frac{9L}{4\pi}\cos(\frac{\pi x}{2L}) - \frac{L}{12\pi}\cos(\frac{3\pi x}{2L}) \\
P_3(x) &= \frac{L^3}{\pi^3}\sin(\frac{\pi x}{2L}) - \frac{L^3}{3\pi^3}\sin(\frac{3\pi x}{2L}) \\
P_4(x) &= -\frac{L^3}{\pi^3}\cos(\frac{\pi x}{2L}) - \frac{L^3}{3\pi^3}\cos(\frac{3\pi x}{2L})
\end{aligned}
\tag{5.41}
$$

5.3.1 Convergence Studies and Result Verification

Considering the circumferential symmetry of the circular shells, the convergence only needs to be checked in the axial direction (i.e., x). In Table 5.3, the first six natural frequencies (Hz) for a two-layered, [0°/90°] laminated cylindrical shell with six truncation schemes (i.e., M = 6, 7, 8, 9, 10, 11, N = 10) are presented. The geometric and material constants of the shell are: R = 1 m, L/R = 5, h/R = 0.1, E_2 = 10 GPa, E_1/E_2 = 15, μ_{12} = 0.27, G_{12} = 0.5E_2, G_{13} = 0.5E_2, G_{23} = 0.2E_2, ρ = 1,700 kg/m^3. The natural frequencies of the shell are calculated by MATAB on a notebook. The configuration of the computer is: Inter Core2 Duo CPU and 2 GB RAM. It is obviously that the modified Fourier series solution has an excellent convergence, and is sufficient accuracy even when only a small number of terms are included in the series expression. The maximum difference between the 'M = 6' and 'M = 11' form results for the F–F and C–C boundary conditions are less than 0.15 and 0.08 %, respectively. Furthermore, from the table, we can see that although the series are truncated as much as 11 × 10, the computing time is less 1.53 s. In addition, convergence of the C–C solutions is faster than the case of F–F boundary conditions. Unless otherwise stated, the truncated number of the displacement expressions will be uniformly selected as M = 11 in the following discussions.

To validate the accuracy and reliability of current method, the current solutions are compared with those reported by other researchers. First, let us consider a

Table 5.3 Convergence of the first six frequencies (Hz) for a [0°/90°] laminated cylindrical shell with F–F and C–C boundary conditions

B.C.	*M*	Mode number						Time (s)
		1	2	3	4	5	6	
F–F	6	3.4476	52.387	54.131	135.37	144.13	146.02	1.11
	7	3.4476	52.387	54.131	135.35	144.13	146.02	1.17
	8	3.4446	52.387	54.127	135.35	144.13	146.02	1.25
	9	3.4446	52.387	54.127	135.34	144.13	146.02	1.35
	10	3.4423	52.387	54.123	135.34	144.13	146.02	1.42
	11	3.4423	52.387	54.123	135.33	144.13	146.02	1.53
C–C	6	91.565	118.86	154.66	160.87	185.97	235.66	1.10
	7	91.514	118.77	154.65	160.87	185.97	235.65	1.19
	8	91.514	118.77	154.65	160.80	185.94	235.54	1.25
	9	91.500	118.74	154.65	160.79	185.94	235.54	1.34
	10	91.501	118.74	154.65	160.77	185.93	235.52	1.42
	11	91.494	118.73	154.65	160.77	185.94	235.51	1.52

Table 5.4 Comparison of the frequency parameters Ω for a [0°/90°/0°] laminated cylindrical shell with different boundary conditions

n	F–F			C–C		
	Messina and Soldatos (1999c)	Present	Error (%)	Messina and Soldatos (1999c)	Present	Error (%)
1	304.13	304.16	0.01	159.31	159.44	0.08
2	26.58	26.56	−0.09	107.71	107.89	0.17
3	74.91	74.78	−0.17	108.05	108.11	0.06
4	142.93	142.51	−0.29	157.23	156.94	−0.18
5	229.74	228.70	−0.45	237.70	236.76	−0.40
7	456.60	452.69	−0.86	460.98	457.16	−0.83
10	917.18	902.24	−1.63	920.32	905.47	−1.61

three-layered, cross-ply [0°/90°/0°] cylindrical shell. The elementally material parameters and geometric properties of the layers of the shell are given as: $L/R = 5$, $h/R = 0.05$, $E_1/E_2 = 25$, $\mu_{12} = 0.25$, $G_{12} = 0.5E_2$, $G_{13} = 0.5E_2$, $G_{23} = 0.2E_2$. Comparisons of the shell with two sets of classical boundary conditions (i.e., F–F and C–C) for the first longitudinal mode (i.e., $m = 1$) and six different circumference wave numbers (i.e., n = 1–5 and 10, n = 6, 8 and 9 were not considered in referential paper) are presented in Table 5.4. From the table, we can see that the present solutions agree very well with results obtained by Messina and Soldatos (1999c). The differences between these two results are very small, and do not exceed 1.63 % for the worst case. The small differences may be caused by a different solution procedure were used by Messina and Soldatos (1999c).

Table 5.5 Comparison of frequency parameters $\Omega = \omega h/\pi\sqrt{\rho/G_{12}}$ for two S–S supported, cross-ply laminated cylindrical shells with different thick-radius ratios (R = 1 m, L/R = 1, E_1/E_2 = 40)

h/R	[0°/90°/90°/0°]			[90°/0°/0°/90°]		
	Present	Ye (2003)	Ich Thinh and Nguyen (2013)	Present	Ye (2003)	Ich Thinh and Nguyen (2013)
0.1	0.0639	0.0646	0.0640	0.0533	0.0527	0.0531
	0.0657	0.0663	0.0657	0.0592	0.0591	0.0591
	0.0789	0.0793	0.0789	0.0710	0.0707	0.0709
0.2	0.1588	0.1638	0.1589	0.1335	0.1302	0.1333
	0.1678	0.1709	0.1683	0.1528	0.1507	0.1527
	0.1727	0.1752	0.1726	0.1593	0.1589	0.1592
0.3	0.2542	0.2630	0.2546	0.2275	0.2188	0.2273
	0.2670	0.2729	0.2669	0.2430	0.2364	0.2428
	0.2788	0.2838	0.2797	0.2701	0.2683	0.2699

The previous example is presented as thin laminated composite cylindrical shell with classical boundary conditions. The validity of the proposed method for vibration analysis of thick laminated composite cylindrical shells will be proved in following examples. In Table 5.5, the detail comparisons between results obtained by present method and those provided by Ye (2003) with 3D elasticity theory as well as Ich Thinh and Nguyen (2013) by the FSDT for certain cross-ply cylindrical shells with S–S boundary conditions are presented, in which two types of lamination schemes ([0°/90°/90°/0°] and [90°/0°/0°/90°]) are included. The material parameters and geometric properties of the layers of the considered shells are assumed to be: R = 1 m, L/R = 1, E_1/E_2 = 40. The comparisons are conducted for thickness-to-radius ratios h/R = 0.1, 0.2, 0.3, respectively. The lowest three frequencies of the shells, which are expressed in terms of non-dimension parameters, $\Omega = \omega h/\pi\sqrt{\rho/G_{12}}$ are computed. It is obvious that the current results match very well with the referential data. The proposed solution is efficient and accurate in predicting nature frequencies of thick laminated cylindrical shells. The differences between the present results and those reported by Ye (2003) are bigger than those relative to Ich Thinh and Nguyen (2013). It is attributed to different shell theories were used in the literature.

Then, a further comparison is performed for laminated composite shells with different boundary conditions and length-to-radius ratios. The used material constants are the same as previous example. Two types of lamination schemes ([0°/90°] and [0°/90°/0°]) and two kinds of length-to-radius ratios (i.e., L/R = 1 and 2) are considered. The fundamental frequency parameters $\Omega = (\omega L^2/100h)\sqrt{\rho/E_2}$ for the shells with thickness-to-radius ratio h/R = 0.2 are calculated. In Table 5.6, comparisons between the present solutions and results reported by Khdeir et al. (1989), Ich Thinh and Nguyen (2013) are presented, in which two sets of classical boundary conditions i.e., S–C and C–C are considered. A good agreement can be

Table 5.6 Comparison of the fundamental frequency parameters $\Omega = (\omega L^2/100h)\sqrt{\rho/E_2}$ of two certain cross-ply laminated cylindrical shells with different length-radius ratios and boundary conditions (R = 1 m, h/R = 0.2)

Lamination schemes	Theories	S–C		C–C	
		L/R = 1	L/R = 2	L/R = 1	L/R = 2
[0°/90°]	HSDT (Khdeir et al. 1989)	0.0938	0.1726	0.1085	0.1928
	FSDT (Khdeir et al. 1989)	0.0893	0.1697	0.1002	0.1876
	CST (Khdeir et al. 1989)	0.1152	0.1841	0.1048	0.2120
	FSDT (Ich Thinh and Nguyen 2013)	0.0823	0.1661	0.0982	0.1737
	Present	0.0921	0.1639	0.0982	0.1738
[0°/90°/0°]	HSDT (Khdeir et al. 1989)	0.1087	0.1972	0.1192	0.2191
	FSDT (Khdeir et al. 1989)	0.1036	0.1945	0.1093	0.2129
	CST (Khdeir et al. 1989)	0.1850	0.2662	0.2049	0.3338
	FSDT (Ich Thinh and Nguyen 2013)	0.1025	0.1950	0.1083	0.2083
	Present	0.1028	0.1991	0.1086	0.2084

seen from the table. The small deviations in the results are caused by different computation methods and shell theories were used in the literature.

5.3.2 *Effects of Shear Deformation and Rotary Inertia*

In this section, effects of the shear deformation and rotary inertia which are neglected in the CST will be investigated. Figures 5.5 and 5.6 show the differences between the lowest three frequency parameters Ω obtained by CST and SDST of a short (R/L = 1), two-layered, [0°/90°] laminated cylindrical shell with different thickness-to-radius ratios (h/R) and orthotropy ratios (E_1/E_2) for F–F and C–C boundary conditions, respectively. Two orthotropy ratios, i.e., E_1/E_2 = 1 and 40, corresponding to isotropic and composite shells are shown in each figure. The thickness-to-radius ratio h/R is varied from 0.001 to 0.2, corresponding to very thin to thick cylindrical shells. As expected, the figures show that the difference between the CST and SDST solutions increases as h/R increases. In addition, we can see that the effects of the shear deformation and rotary inertia increase as the orthotropy ratio (E_1/E_2) increases. From Fig. 5.5, we can see that when h/R is less than 0.01, the maximum difference between the frequency parameters Ω obtained by CST and SDST is less than 0.21 % for the worst case. However, when h/R is equal to 0.1, the maximum difference can be as many as 3.75 and 4.3 % for the cylindrical shell with orthotropy ratios of E_1/E_2 = 1 and E_1/E_2 = 40, respectively. Figure 5.5 also shows that the maximum differences between these two results can be as many as 8.12 and 10.22 % for a thickness-to-radius ratio of 0.2. Figure 3.6 shows that the maximum

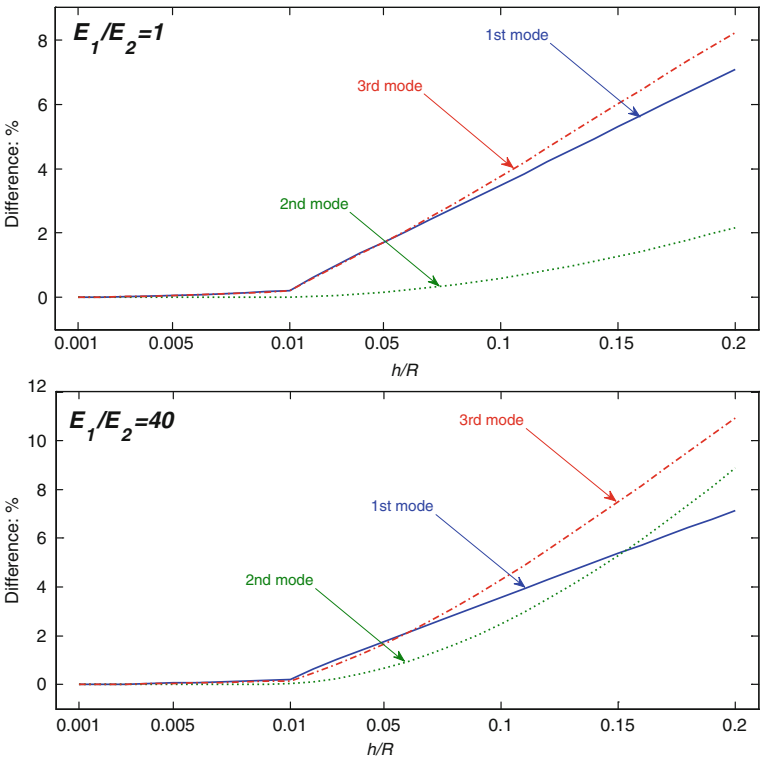

Fig. 5.5 Differences between the lowest three frequency parameters Ω obtained by CST and SDST for a short [0°/90°] laminated cylindrical shell with F–F boundary conditions (R/L = 1)

difference between these CST and SDST results can be as many as 16.3 and 59.9 % for the C–C cylindrical shell with orthotropy ratios of E_1/E_2 = 1 and E_1/E_2 = 40, respectively. In such case, the CST results are utterly inaccurate.

For the sake of completeness, Figs. 5.7 and 5.8 show the similar studies for a long (R/L = 5), [0°/90°] laminated cylindrical shell. Constantly, the effects of shear deformation and rotary inertia increase with thickness-to-span length ratio increases. Comparing Figs. 5.7 and 5.8 with Figs. 5.5 and 5.6, we can find that the effects of shear deformation and rotary inertia decrease as length-to-radius ratio increases. The maximum difference between the CST and SDST results is less than 7.5 % for the worst case, which is only one eighth of those of cylindrical shell with length-to-radius ratio L/R = 1. These investigations show that the CST is only applicable for thin cylindrical shells as well as the long moderately thick ones. For cylindrical shells with higher thickness ratios or smaller length-to-radius ratios, both shear deformation and rotary inertia effects should be included in the calculation.

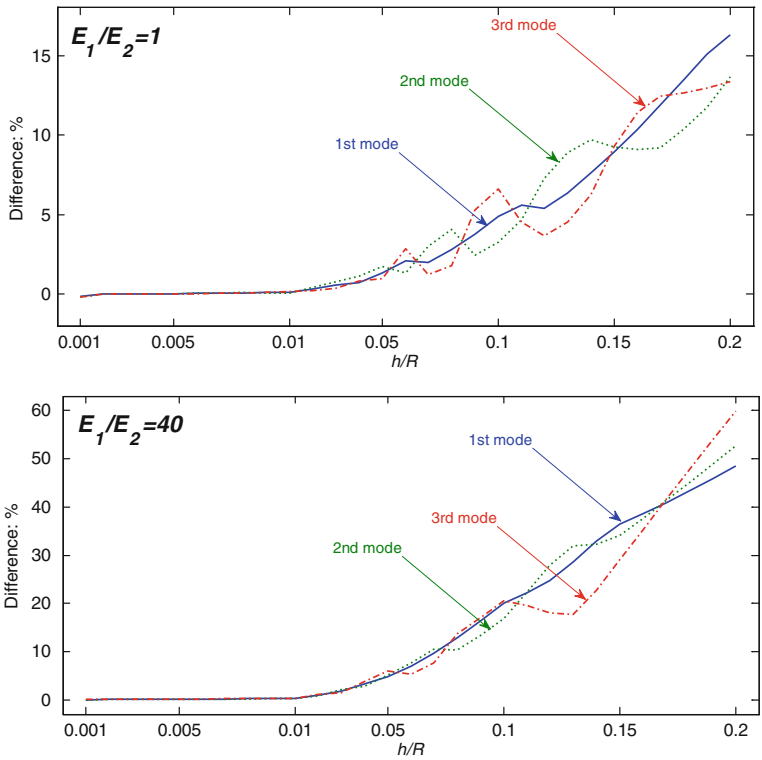

Fig. 5.6 Differences between the lowest three frequency parameters Ω obtained by CST and SDST for a short [0°/90°] laminated cylindrical shell with C–C boundary conditions (R/L = 1)

5.3.3 *Laminated Closed Cylindrical Shells with General End Conditions*

First, let us consider a three-layered, [0°/90°/0°] cylindrical shell with various thickness-to-radius ratios. The material properties and geometric constants of the layers of the shell are: E_1/E_2 = 15, R = 1 m, L/R = 2. In Table 5.7, the lowest four frequency parameters Ω for the shell are presented, in which six sets of classical boundary combinations (i.e., F–F, F–S, F–C, S–S, S–C and C–C) and five kinds of thickness-to-radius ratios (h/R = 0.01, 0.02, 0.05, 0.1 and 0.15) are included in the table. It can be seen from the table that the frequency parameters increase in general as the thickness-radius ratio increases. The second observation that needs to be made here is that the effects of thickness-to-radius ratio are much higher for the thicker cylindrical shells than it is for the thinner ones. In addition, it is obviously that boundary conditions have a conspicuous effect on the vibration frequencies of the shell. Increasing the restraint stiffness always results in increment of the frequency parameters.

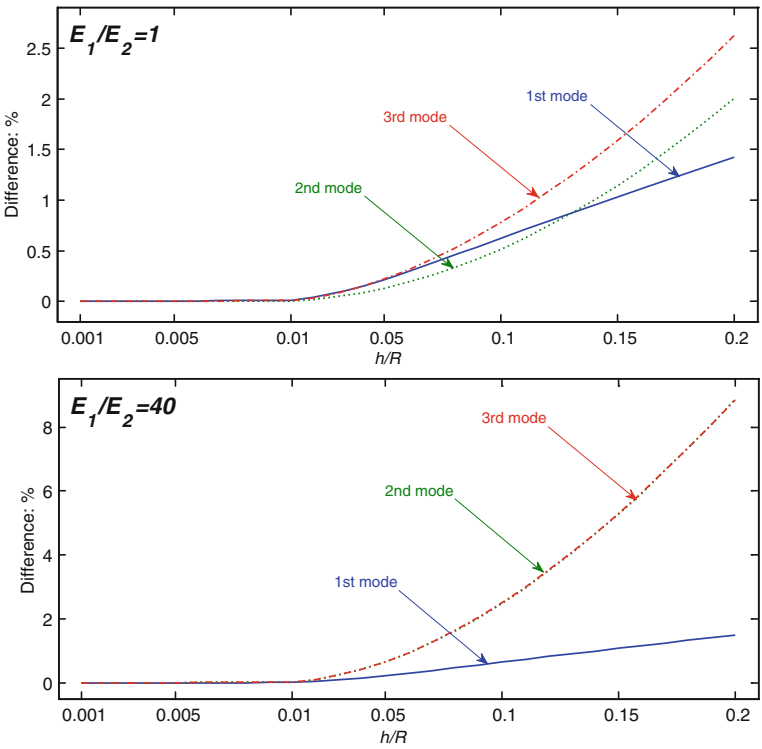

Fig. 5.7 Differences between the lowest three frequency parameters Ω obtained by CST and SDST for a long [0°/90°] laminated cylindrical shell with F–F boundary conditions (R/L = 5)

Table 5.8 shows the lowest four frequency parameters Ω of a moderately thick cylindrical shell with different lamination schemes for various boundary conditions. Five lamination schemes, i.e., [0°], [90°], [0°/90°], [0°/90°/0°] and [0°/90°/0°/90°] are studied for all aforementioned boundary conditions (see Table 5.7). The geometric and material constants used in the study are: R = 1 m, L/R = 1, h/R = 0.1, E_1/E_2 = 15. When the shell with F–F, F–S and F–C boundary conditions, the [90°] lamination scheme yields higher frequency parameter than those of [0°], [0°/90°], [0°/90°/0°] and [0°/90°/0°/90°] (except the fundamental mode). For other boundary conditions, the frequency parameters of [90°] are the smallest among the five lamination schemes. Furthermore, the [0°] lamination scheme yields significantly lower frequency parameters than those of [0°/90°/0°]. The similar comparison results can be seen for [0°/90°] and [0°/90°/0°/90°] lamination schemes.

The effects of length-to-radius ratio on frequency parameters are also investigated. Table 5.9 shows the lowest four frequency parameters Ω for a two-layered, unsymmetrically laminated cross-ply cylindrical shell ([0°/90°]) with various length-to-radius ratios and different sets of boundary conditions. The shell is assumed to be made of composite layers with following geometric and material constants:

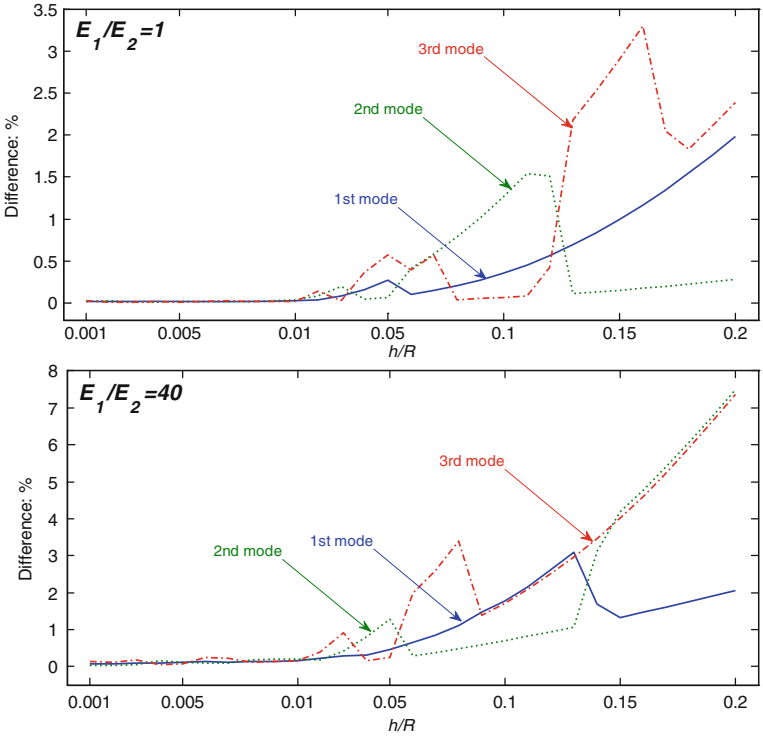

Fig. 5.8 Differences between the lowest three frequency parameters Ω obtained by CST and SDST for a long [0°/90°] laminated cylindrical shell with C–C boundary conditions ($R/L = 5$)

$R = 1$ m, $h/R = 0.05$, $E_1/E_2 = 15$. It is obviously that the length-to-radius ratio has a great influence on the vibration of the shell. The frequency parameters decrease when the length-radius ratio is increased.

The following numerical analysis is conducted to investigate the influence of fiber orientations on the frequency parameters Ω of laminated cylindrical shells. Let us consider a three-layered [0°/ϑ/0°] cylindrical shell with varying boundary conditions. The shell is modeled as both the top and bottom layers are of uniform principal direction which is paralleled to x-axis whilst the included angle between the fiber orientation of the middle layer and x-axis is changed from 0° to 180° step-by-step. In Fig. 5.9, the first three frequency parameters Ω for the shell with three types of boundary conditions (i.e., SD–SD, S–S and C–C) are plotted, respectively. The following geometric and material properties are used in the analysis: $R = 1$ m, $L/R = 2$, $h/R = 0.05$, $E_1/E_2 = 15$. Many interesting characteristics can be observed from the figure. The first observation is that all the figures are symmetrical about central line (i.e., $\vartheta = 90°$). The second observation is that the frequency parameter traces in all cases climb up and then decline, and reach their crests around $\vartheta = 50°$ when ϑ is increased from 0 to 90° except the second mode of SD-SD boundary

Table 5.7 Frequency parameters Ω for a [0°/90°/0°] laminated cylindrical shell with various thickness-to-radius ratios and boundary conditions (R = 1 m, L/R = 2, E_1/E_2 = 15)

h/R	Mode	Boundary conditions					
		F–F	F–S	F–C	S–S	S–C	C–C
0.01	1	0.6924	47.444	47.887	91.228	93.711	96.460
	2	3.8252	49.853	50.482	94.879	97.010	99.436
	3	5.7572	55.831	56.111	97.776	100.42	103.28
	4	10.818	65.872	66.601	107.00	108.73	110.75
0.02	1	0.6913	31.185	31.833	59.048	61.749	64.919
	2	3.8242	34.505	35.361	62.322	65.184	68.399
	3	5.7498	38.063	38.471	64.959	67.227	70.009
	4	10.812	50.185	51.009	76.562	79.194	82.038
0.05	1	0.6868	17.397	18.321	34.303	37.189	40.825
	2	3.8178	20.540	21.570	34.342	37.371	40.972
	3	5.7149	23.205	23.788	41.782	44.120	47.219
	4	10.772	33.448	34.046	43.830	46.327	49.130
0.10	1	0.6794	11.010	12.122	22.277	25.089	28.433
	2	3.7968	13.105	13.921	23.925	26.512	29.471
	3	5.6384	16.769	17.456	27.431	29.741	32.624
	4	10.638	21.360	21.857	34.142	35.582	37.150
0.15	1	0.6720	8.053	9.1254	17.725	19.981	22.435
	2	3.7633	11.216	11.919	18.755	20.955	23.424
	3	5.5395	11.945	12.638	23.400	24.722	26.135
	4	10.431	20.377	20.789	25.035	26.676	28.591

conditions, in which the maximum frequency parameters occur around $\vartheta = 60°$. In addition, it is obvious that, the second frequency parameters almost equal to the third ones when $\vartheta = 20°$ and the differences between the first frequency parameters and the second ones are very small for a fiber orientation of 90°.

Figure 5.10 performs the similar study for a two-layered [0°/ϑ] cylindrical shell. The similar characteristics observed in Fig. 5.9 can be found in this figure as well. The different observation is that the variation tendencies of the frequency parameters are more complicated than those of Fig. 5.9. It may be due to the shell is unsymmetrically laminated.

Laminated composite cylindrical shells with elastically restrained edges are widely encountered in engineering practices. The vibration analyses of these shells are necessary and of great significance. There are infinite types of possible combinations of elastic boundary conditions at the two edges of the cylindrical shells, and it is impossible to undertake an all-encompassing survey of them. Therefore, in this paper we choose three typical uniform elastic restraint conditions that are defined as follows (at $x = 0$):

Table 5.8 Frequency parameters Ω for a moderately thick laminated cylindrical shell with various lamination schemes and boundary conditions (R = 1 m, L/R = 1, h/R = 0.1, E_1/E_2 = 15)

Lamination schemes	Mode	Boundary conditions					
		F–F	F–S	F–C	S–S	S–C	C–C
[0°]	1	0.1973	4.6489	6.0143	12.092	14.494	16.976
	2	0.7703	5.0847	6.3089	12.366	14.746	17.220
	3	1.8917	5.6701	6.8472	12.575	14.863	17.242
	4	2.1636	7.0632	7.8891	13.256	15.555	17.986
[90°]	1	0.1993	5.3648	5.5490	11.244	11.865	12.571
	2	2.8163	7.9426	8.0825	11.354	11.956	12.691
	3	2.8341	8.1412	8.2330	15.357	15.793	16.357
	4	7.5175	13.087	13.667	16.394	16.750	17.132
[0°/90°]	1	0.1993	5.7888	5.9648	11.441	12.140	13.279
	2	1.3637	5.8632	5.9869	12.411	13.062	14.113
	3	2.0319	8.1790	8.2594	12.558	13.185	14.199
	4	3.7740	8.3929	8.5320	15.247	15.756	16.563
[0°/90°/0°]	1	0.1990	4.9791	6.3003	12.512	14.780	17.130
	2	0.9487	5.5288	6.7570	12.936	15.140	17.446
	3	1.9630	6.3494	7.4064	13.549	15.578	17.699
	4	2.6585	8.3430	9.0301	14.484	16.444	18.538
[0°/90°/0°/90°]	1	0.1992	5.8999	6.4928	12.256	13.833	15.742
	2	1.9420	6.8706	7.3300	12.748	14.224	15.985
	3	2.3103	8.4126	8.7915	14.384	15.745	17.451
	4	5.3078	10.520	10.806	16.692	17.654	18.795

E^1: The normal direction is elastically restrained ($u \neq 0$, $v = w = \phi_x = \phi_\theta = 0$), i.e., $k_u = \Gamma$;
E^2: The transverse direction is elastically restrained ($w \neq 0$, $u = v = \phi_x = \phi_\theta = 0$), i.e., $k_w = \Gamma$;
E^3: The rotation is elastically restrained ($\phi_x \neq 0$, $u = v = w = \phi_\theta = 0$), i.e., $K_x = \Gamma$.

Table 5.10 shows the lowest two frequency parameters Ω of a two-layered [0°/ϑ] cylindrical shell with different restrain parameters Γ and fiber orientations. Four different lamination schemes, i.e., ϑ = 0°, 30°, 60° and 90° are performed in the calculation. The shell parameters used are R = 1 m, L/R = 3, h/R = 0.05, E_1/E_2 = 15. The shell is clamped at the edge of $x = L$ and with elastic boundary conditions at the other edge. The table shows that increasing restraint rigidities in the normal and transverse directions have very limited effects on the frequency parameters of the shell. When the normal restrained rigidity is varied from $10^{-1} * D$ to $10^3 * D$, the maximum increment in the table is less than 2.49 % for all cases. The further observation from the table is that for the shell with lamination scheme of [0°],

Table 5.9 The lowest four frequency parameters Ω for a [0°/90°] laminated cylindrical shell with various length-to-radius ratios and boundary conditions (R = 1 m, h/R = 0.05, E_1/E_2 = 15)

L/R	Mode	Boundary conditions					
		F–F	F–S	F–C	S–S	S–C	C–C
1	1	0.2032	8.8400	8.9230	16.894	17.614	18.718
	2	1.4017	9.9271	9.9750	17.726	18.459	19.555
	3	2.1356	10.866	10.982	18.653	19.283	20.253
	4	3.9373	13.394	13.428	21.924	22.558	23.462
2	1	0.6868	20.615	20.618	36.090	36.479	36.953
	2	5.6072	20.664	20.676	40.438	40.710	41.043
	3	6.8179	31.790	31.795	43.913	44.325	44.813
	4	15.751	33.172	33.173	54.095	54.271	54.483
3	1	1.2663	29.385	29.487	58.491	58.637	58.800
	2	12.617	39.266	39.324	65.558	65.780	66.026
	3	14.005	48.125	48.161	77.299	77.366	77.439
	4	35.441	66.797	67.810	97.770	99.680	101.60
4	1	1.8621	38.500	38.718	86.300	86.330	86.363
	2	22.430	61.348	61.495	86.869	86.961	87.057
	3	23.895	65.943	66.010	128.66	128.67	128.68
	4	63.007	94.226	94.610	133.41	134.70	134.98
5	1	2.4535	49.307	49.581	107.98	107.99	107.99
	2	35.047	72.760	73.053	120.62	120.62	120.62
	3	36.550	100.78	100.84	167.63	167.65	167.70
	4	98.451	127.71	127.81	172.83	173.61	174.42

the effect of the rotation direction restraint rigidity is more significant. When the rotation restraint rigidity is varied from $10^{-1} * D$ to $10^{3} * D$, the increments of the first and second modes can be 5.57 and 4.99 %, respectively).

Table 5.11 shows similar studies for the shell with F boundary conditions at the edge of $x = L$. The table reveals that the restraint rigidity at normal direction has large effects on the frequency parameters of all the lamination schemes. When the normal direction restraint rigidity is varied from $10^{-1} * D$ to $10^{3} * D$, the increments of these four lamination schemes for the first and second modes can be (1,037, 1,087, 1,118, 1,103 %) and (359, 393, 654, 879 %), respectively. This table also shows that the increments of the restraint rigidities in the transverse and rotation directions have very limited effects on the frequency parameters of the shell, with maximum increment less than 2.73 % in all cases when the rotation restrained rigidity is varied from $10^{-1} * D$ to $10^{4} * D$. From the two tables, it is obvious that the effects of elastic restraint rigidity on the frequency parameters of laminated cylindrical shells is varied with mode sequences, lamination schemes and spring components.

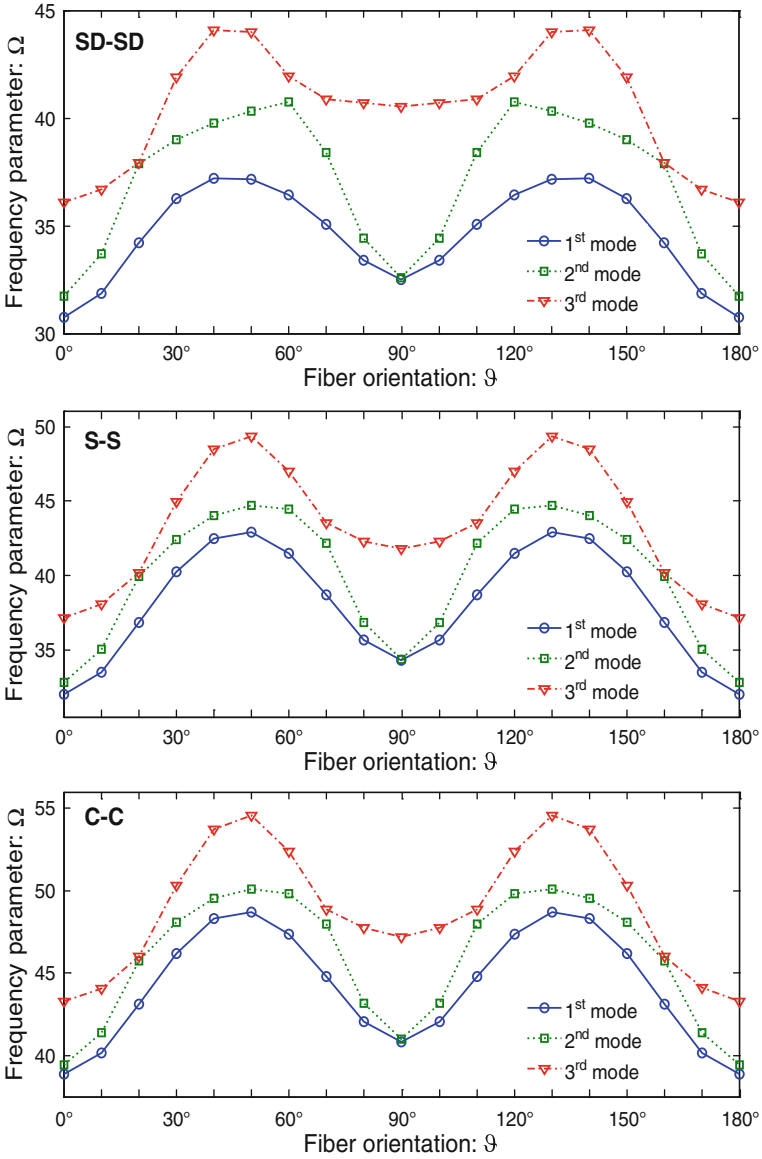

Fig. 5.9 Influence of fiber orientations on frequency parameters Ω of a three-layered [0°/ϑ/0°] cylindrical shell

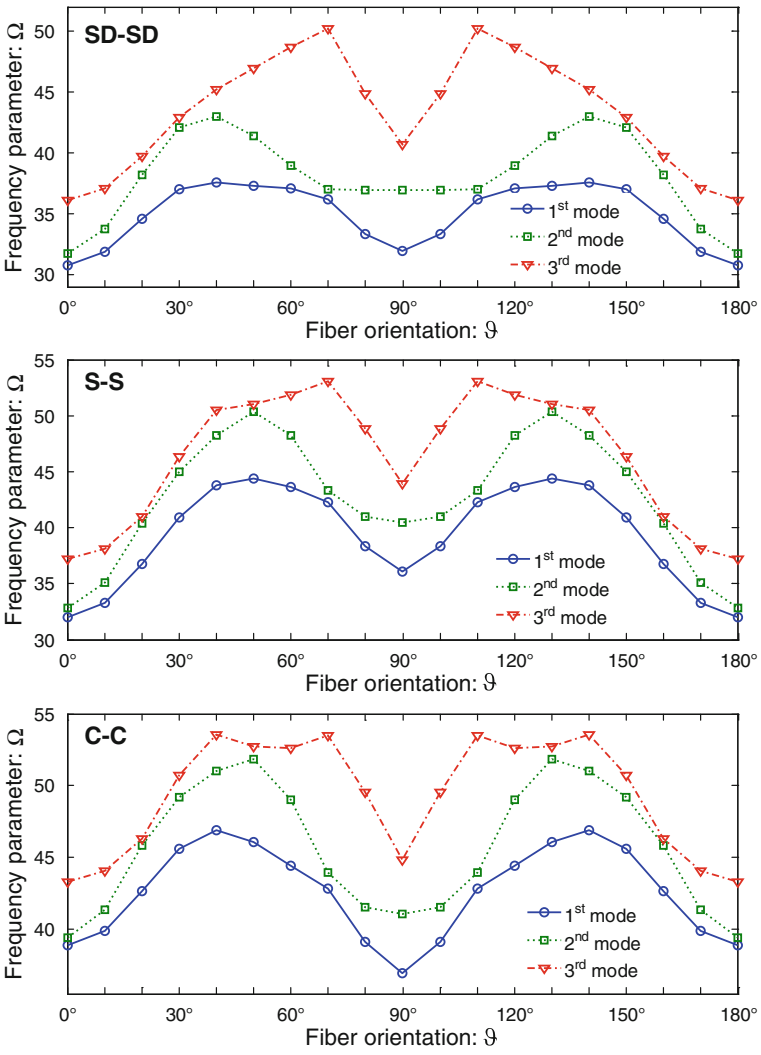

Fig. 5.10 Influence of fiber orientations on frequency parameters Ω of a two-layered [0°/ϑ] cylindrical shell

5.3.4 Laminated Closed Cylindrical Shells with Intermediate Ring Supports

Cylindrical shells with intermediate ring supports are widely used in engineering practices, such as pipelines for undersea transmission cables, irrigation pipes, and household water pipes. Without these intermediate supports, these structures may undergo large deformation, and violent vibration due to their low stiffness, and will

Table 5.10 The first two frequency parameters Ω for a two-layered [0°/ϑ] cylindrical shell with different restrain parameters Γ and fiber orientations (R = 1 m, L/R = 3, h/R = 0.05, E_1/E_2 = 15)

ϑ	Γ	E^1 − C		E^2 − C		E^3 − C	
		1	2	1	2	1	2
0°	$10^{-1} \times D$	54.351	57.998	55.146	58.474	53.390	56.641
	$10^{0} \times D$	54.351	57.998	55.178	58.460	53.905	57.149
	$10^{1} \times D$	54.358	58.002	55.265	58.548	55.473	58.649
	$10^{2} \times D$	54.418	58.037	55.808	58.988	56.256	59.370
	$10^{3} \times D$	54.871	58.311	56.282	59.393	56.366	59.470
30°	$10^{-1} \times D$	68.056	68.804	69.239	72.454	68.847	72.258
	$10^{0} \times D$	68.057	68.805	69.257	72.582	69.142	72.550
	$10^{1} \times D$	68.061	68.818	69.321	72.689	70.063	73.498
	$10^{2} \times D$	68.108	68.946	69.804	73.229	70.536	74.008
	$10^{3} \times D$	68.498	69.954	70.441	73.914	70.604	74.082
60°	$10^{-1} \times D$	64.869	73.191	70.924	75.311	71.434	75.639
	$10^{0} \times D$	64.869	73.192	70.923	75.308	71.457	75.663
	$10^{1} \times D$	64.891	73.198	70.944	75.316	71.518	75.726
	$10^{2} \times D$	65.077	73.251	71.095	75.431	71.544	75.752
	$10^{3} \times D$	66.487	73.688	71.420	75.663	71.548	75.755
90°	$10^{-1} \times D$	55.862	62.395	58.534	65.692	58.644	65.790
	$10^{0} \times D$	55.863	62.396	58.535	65.693	58.687	65.850
	$10^{1} \times D$	55.875	62.422	58.546	65.703	58.770	65.976
	$10^{2} \times D$	56.000	62.632	58.611	65.783	58.796	66.019
	$10^{3} \times D$	56.833	63.889	58.747	65.954	58.800	66.026

eventually lead to failure. The vibration analyses of these shells are necessary and particularly important. However, cylindrical shells with intermediate supports have received limited attention. Vibrations of laminated cylindrical shells with arbitrary intermediate ring supports will be considered in the subsequent analysis.

As shown in Fig. 5.11, a laminated cylindrical shell restrained by arbitrary intermediate ring supports is chosen as the analysis model. a_i represents the position of the i'th ring support along the axial direction of the shell. The displacement fields in the position of the ring support satisfy $w_0\,(a_i, \theta) = 0$ (Swaddiwudhipong et al. 1995; Zhang and Xiang 2006). This condition can be readily obtained by introducing a set of continuously distributed linear springs at the position of each ring support to restrict the displacement in radial direction and setting the stiffness of these springs equal to infinite (which is represented by a very large number, $10^7\ D$). Thus, the potential energy (P_{irs}) stored in the ring supported springs can be depicted as:

$$P_{irs} = \frac{1}{2}\int_{\theta}\left\{\sum_{i=1}^{N_i} k_w^i w(a_i,\theta)^2\right\} R d\theta \tag{5.42}$$

Table 5.11 The first two frequency parameters Ω for a two-layered [0°/ϑ] cylindrical shell with different restrain parameters Γ and fiber orientations (R = 1 m, L/R = 3, h/R = 0.05, E_1/E_2 = 15)

ϑ	Γ	E^1 − F		E^2 − F		E^3 − F	
		1	2	1	2	1	2
0°	$10^{-1} \times D$	1.8409	5.1377	27.916	30.197	27.470	29.729
	$10^{0} \times D$	5.5480	5.8210	27.918	30.206	27.585	29.860
	$10^{1} \times D$	8.5948	10.415	27.936	30.234	27.925	30.281
	$10^{2} \times D$	12.470	20.970	28.021	30.381	28.090	30.506
	$10^{3} \times D$	20.946	23.605	28.099	30.515	28.114	30.539
30°	$10^{-1} \times D$	1.8409	5.2805	29.420	35.936	29.589	36.424
	$10^{0} \times D$	5.6731	5.8208	29.422	35.937	29.622	36.470
	$10^{1} \times D$	8.6521	11.695	29.439	35.986	29.730	36.625
	$10^{2} \times D$	13.358	21.687	29.579	36.274	29.788	36.715
	$10^{3} \times D$	21.870	26.044	29.755	36.636	29.796	36.728
60°	$10^{-1} \times D$	1.8409	4.4993	34.774	36.036	34.893	36.107
	$10^{0} \times D$	4.9467	5.8205	34.776	36.037	34.920	36.112
	$10^{1} \times D$	8.1479	13.429	34.784	36.040	34.995	36.126
	$10^{2} \times D$	14.868	21.309	34.846	36.064	35.029	36.133
	$10^{3} \times D$	22.433	33.538	34.980	36.111	35.034	36.134
90°	$10^{-1} \times D$	1.8409	3.8049	29.401	39.298	29.389	39.269
	$10^{0} \times D$	4.3293	5.8205	29.401	39.298	29.414	39.284
	$10^{1} \times D$	7.7880	13.965	29.404	39.299	29.466	39.313
	$10^{2} \times D$	15.478	20.351	29.424	39.306	29.484	39.323
	$10^{3} \times D$	22.150	37.252	29.468	39.319	29.486	39.324

where N_i is the amount of ring supports. k_w^i denotes the set of ring supported springs distributed at $x = a_i$. By adding the potential energy P_{irs} stored in the ring supported springs in the Lagrangian energy functional and applying the weak form solution procedure, the characteristic equation for the shell with arbitrary end conditions and ring supports can be readily obtained.

To validate the present analysis, results for C–F isotropic cylindrical shells with one ring support are compared with others in the literature. In Table 5.12, comparisons of the first three longitudinal modal (i.e., m = 1, 2, 3) non-dimensional frequency parameters $\Omega = \omega R\sqrt{\rho(1-\mu^2)/E}$ of an isotropic cylindrical shell with one (a_1/L = 1/2) ring supports are presented. The lowest four circumference wave numbers (i.e., n = 1, 2, 3, 4) are considered in the analysis. The material and geometrical properties of the shell are given as: L/R = 50, μ = 0.3. The comparisons are conducted for thickness ratios h/R = 0.005, 0.05, respectively. The results reported by Swaddiwudhipong et al. (1995) are considered in the comparison. A good agreement can be seen from the table. The small deviations in the results are caused by different computation methods and shell theories are used in the literature.

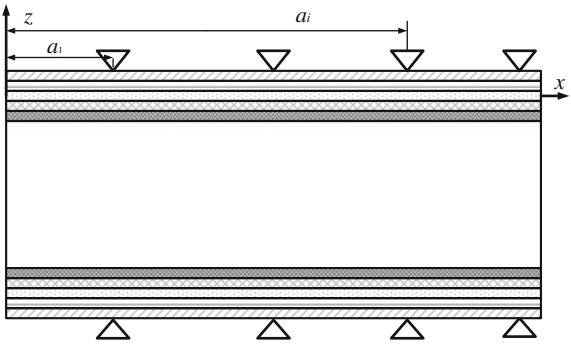

Fig. 5.11 Schematic diagram of a laminated cylindrical shell with intermediate ring supports

Table 5.12 Comparison of frequency parameters $\Omega = \omega R\sqrt{\rho(1-\mu^2)/E}$ of a C–F cylindrical shell with one (a_1/L = 1/2) ring support (L/R = 50, μ = 0.3)

h/R	n	Swaddiwudhipong et al. (1995)			Present		
		m = 1	m = 2	m = 3	m = 1	m = 2	m = 3
0.005	1	0.00267	0.01599	0.02268	0.00265	0.01598	0.02243
	2	0.00394	0.00651	0.00847	0.00397	0.00652	0.00845
	3	0.01097	0.01125	0.01155	0.01097	0.01126	0.01156
	4	0.02101	0.02108	0.02114	0.02101	0.02108	0.02115
0.05	1	0.00267	0.01600	0.02269	0.00267	0.01601	0.02245
	2	0.03876	0.03930	0.03975	0.03871	0.03928	0.03973
	3	0.10950	0.10980	0.10990	0.10912	0.10935	0.10957
	4	0.21000	0.21020	0.21040	0.20850	0.20873	0.20894

The influence of ring support location on the frequencies of a four-layered, [45°/−45°/45°/−45°] cylindrical shell with one intermediate ring support is also investigated. The material and geometric constants of the layers of the shell are: L/R = 10, h/R = 0.1, E_1/E_2 = 25, μ_{12} = 0.27, $G_{12} = 0.5E_2$, $G_{13} = 0.5E_2$, $G_{23} = 0.2E_2$. In Fig. 5.12, variations of the lowest three longitudinal model (n = 1, m = 1, 2, 3) frequency parameters Ω of the considered cylindrical shell against the ring support location parameter a/L are depicted. Four types of end conditions included in the presentation are: F–C, C–F, S–S, and C–C. It is obvious that the frequency parameters of the shell significantly affected by the location of the ring support, and this effect varies with the end conditions. For a cylindrical shell with symmetrical boundary conditions imposed on both ends, such as S–S and C–C boundary conditions, the frequency parameter curves are symmetrical about the center line of the figure (i.e., a/L = 0.5). For a cylindrical shell with unsymmetrical end conditions, such as F–C and C–F boundary conditions, the frequency parameter curves are not symmetrical about the center line of the figure. Figures 5.13 and 5.14 show the similar studies for the second and third circumference numbers (n = 2, 3), respectively. Comparing with Fig. 5.12, it can be seen that the influence of the ring

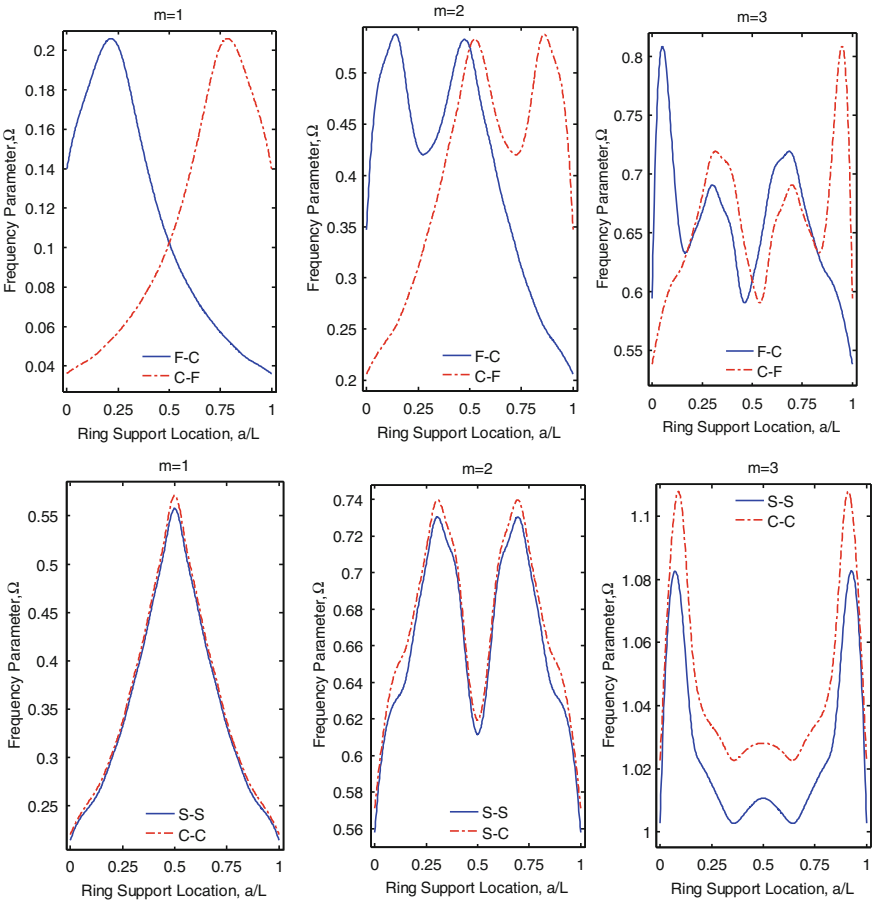

Fig. 5.12 Variations of frequency parameters Ω versus ring location (a/L) for a $[45°/-45°]_2$ laminated cylindrical shell with one intermediate ring support (n = 1)

support location varies with circumference numbers as well. In addition, the amount of the peak values of a frequency parameter curve is in direct proportion to the longitudinal mode number.

5.4 Vibration of Laminated Open Cylindrical Shells

Composite laminated open cylindrical shells have a wide range of engineering applications, particularly in aerospace crafts, military hardware and civil constructions. Table 5.2 shows that thick cylindrical shells can have 24 possible classical boundary conditions at each edge. This leads to 576 combinations of

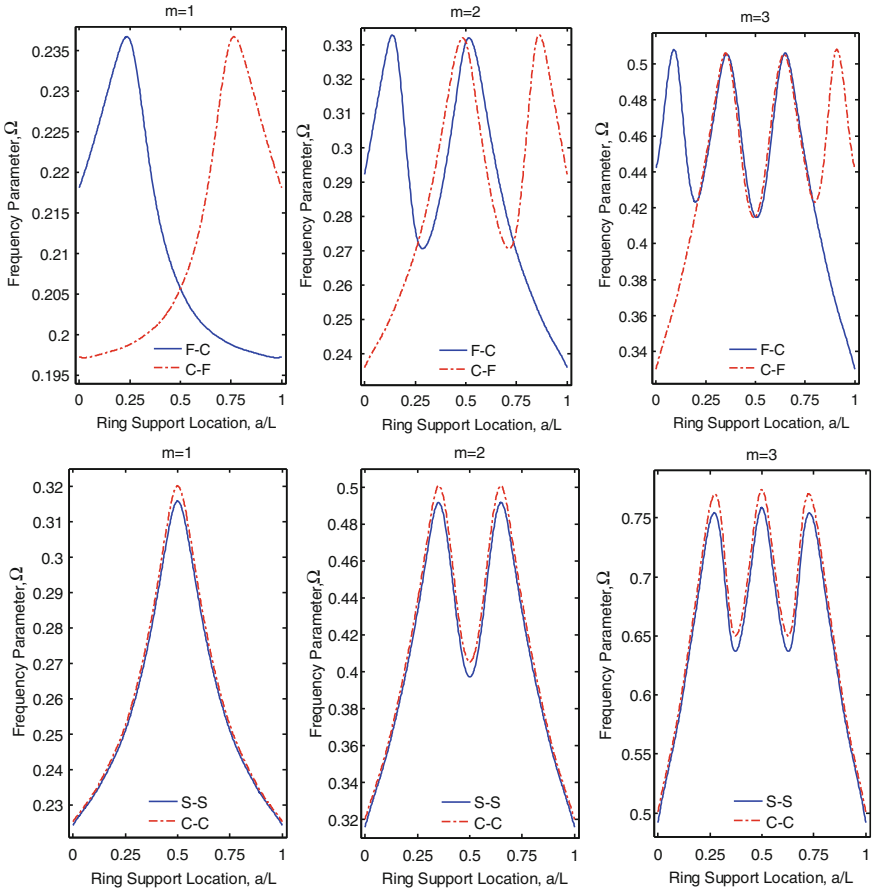

Fig. 5.13 Variations of frequency parameters Ω versus ring location (*a*/*L*) for a $[45°/-45°]_2$ laminated cylindrical shell with one intermediate ring support ($n = 2$)

boundary conditions when a cylindrical shell is closed. When the shells are open, this yields a higher number of combinations of boundary conditions for such shells.

In comparing to laminated closed cylindrical shells, information available for the vibrations of the shallow and deep open ones is very limited despite their practical importance. The most likely reason for this lacuna lies in the analytical difficulties involved: for a completely closed shell such as circular cylindrical, circular conical and spherical shells, the assumed 2D displacement field can be reduced to a quasi 1D problem through Fourier decomposition of the circumferential wave motion. However, for an open shell, the assumption of whole periodic wave numbers in the circumferential direction is inappropriate, and thus, a set of complete two-dimensional analysis is required and resort must be made to a full two-dimensional solution scheme. Such a scheme will inevitably be complicated further by the

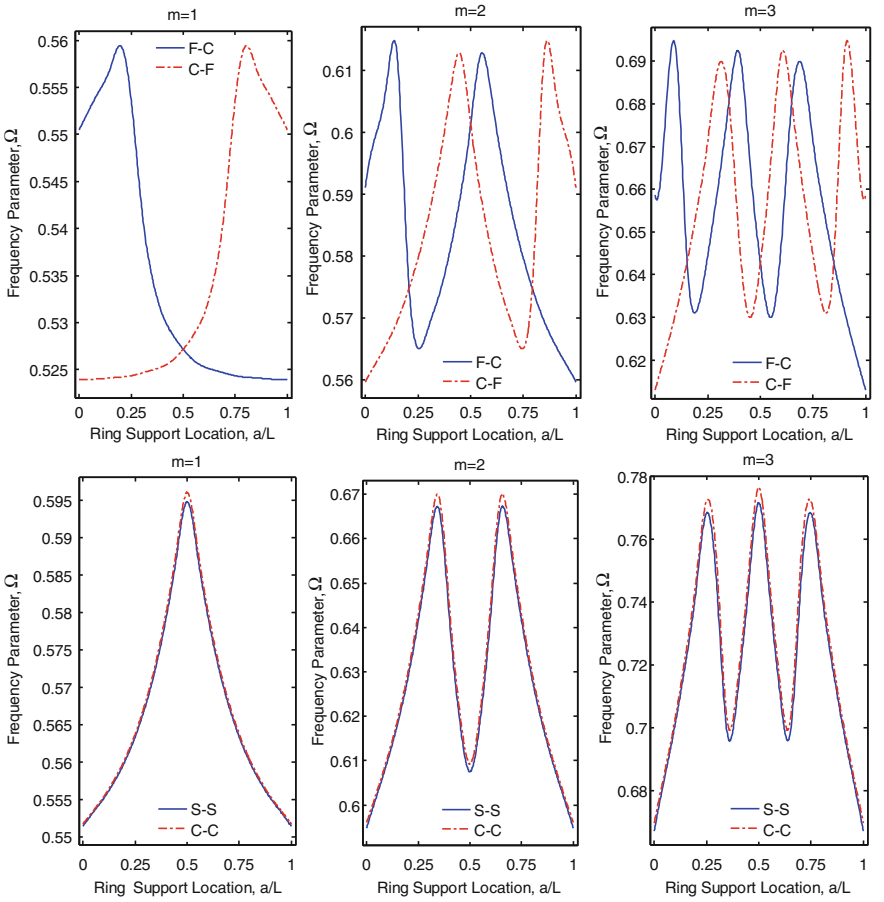

Fig. 5.14 Variations of frequency parameters Ω versus ring location (a/L) for a $[45°/-45°]_2$ laminated cylindrical shell with one intermediate ring support (n = 3)

dependence of the circumferential arc length on its meridional location (Bardell et al. 1998). This forms a major deterrent so that the analyses of open shells have not been widely available.

In this section, we consider free vibration of laminated deep open cylindrical shells. As was done previously for the closed cylindrical shells, only solutions in the framework of SDST which neglecting the effects of the deepness term z/R (i.e., Eq. (5.26)) are considered in this section. Under the modified Fourier series framework, regardless of boundary conditions, each displacement and rotation component of a laminated open cylindrical shell is expanded as a two-dimensional modified Fourier series as:

$$
\begin{aligned}
u(x,\theta) &= \sum_{m=0}^{M}\sum_{n=0}^{N} A_{mn}\cos\lambda_m x\cos\lambda_n\theta + \sum_{l=1}^{2}\sum_{n=0}^{N} a_{\ln}P_l(x)\cos\lambda_n\theta \\
&\quad + \sum_{l=1}^{2}\sum_{m=0}^{M} b_{lm}P_l(\theta)\cos\lambda_m x \\
v(x,\theta) &= \sum_{m=0}^{M}\sum_{n=0}^{N} B_{mn}\cos\lambda_m x\cos\lambda_n\theta + \sum_{l=1}^{2}\sum_{n=0}^{N} c_{\ln}P_l(x)\cos\lambda_n\theta \\
&\quad + \sum_{l=1}^{2}\sum_{m=0}^{M} d_{lm}P_l(\theta)\cos\lambda_m x \\
w(x,\theta) &= \sum_{m=0}^{M}\sum_{n=0}^{N} C_{mn}\cos\lambda_m x\cos\lambda_n\theta + \sum_{l=1}^{2}\sum_{n=0}^{N} e_{\ln}P_l(x)\cos\lambda_n\theta \\
&\quad + \sum_{l=1}^{2}\sum_{m=0}^{M} f_{lm}P_l(\theta)\cos\lambda_m x \\
\phi_x(x,\theta) &= \sum_{m=0}^{M}\sum_{n=0}^{N} D_{mn}\cos\lambda_m x\cos\lambda_n\theta + \sum_{l=1}^{2}\sum_{n=0}^{N} g_{\ln}P_l(x)\cos\lambda_n\theta \\
&\quad + \sum_{l=1}^{2}\sum_{m=0}^{M} h_{lm}P_l(\theta)\cos\lambda_m x \\
\phi_\theta(x,\theta) &= \sum_{m=0}^{M}\sum_{n=0}^{N} E_{mn}\cos\lambda_m x\cos\lambda_n\theta + \sum_{l=1}^{2}\sum_{n=0}^{N} i_{\ln}P_l(x)\cos\lambda_n\theta \\
&\quad + \sum_{l=1}^{2}\sum_{m=0}^{M} j_{lm}P_l(\theta)\cos\lambda_m x
\end{aligned}
\tag{5.43}
$$

where $\lambda_m = m\pi/L$ and $\lambda_n = n\pi/\theta_0$. A_{mn}, B_{mn}, C_{mn}, D_{mn} and E_{mn} are expansion coefficients of standard cosine Fourier series. a_{ln}, b_{lm}, c_{ln}, d_{lm}, e_{ln}, f_{lm} g_{ln}, h_{lm}, i_{ln} and j_{lm} are the corresponding supplement coefficients. $P_l\,(x)$ and $P_l\,(\theta)$ denote two sets auxiliary polynomial functions introduced to remove all the discontinuities potentially associated with the first-order derivatives at the boundaries of $x = 0$, $x = L$ and $\theta = 0$, $\theta = \theta_0$, respectively. These auxiliary functions are in the similar forms as Eq. (5.41).

For a general open cylindrical shell, there exist four boundaries, i.e., $x = 0$, $x = L$, $\theta = 0$ and $\theta = \theta_0$. For the sake of brevity, a four-letter character is employed to represent the boundary condition of an open cylindrical shell, such as FCSC identifies the shell with F, C, S and C boundary conditions at boundaries $x = 0$, $\theta = 0$, $x = L$ and $\theta = \theta_0$, respectively. Unless otherwise stated, the natural frequencies of the considered shells are expressed as frequency parameter as $\Omega =$

$(\omega L^2/h)\sqrt{\rho/E_2}$ and the material properties of the layers of open cylindrical shells under consideration are taken as: E_2 = 10 GPa, E_1/E_2 = open, μ_{12} = 0.25, $G_{12} = G_{13} = 0.5E_2$, $G_{23} = 0.2E_2$, ρ = 1,450 kg/m^3.

5.4.1 Convergence Studies and Result Verification

Table 5.13 shows the convergence and comparison studies of frequency parameters $\Omega = \omega L^2/h\sqrt{\rho/E_1}$ for a four-layered, [−60°/60°/60°/−60°] open cylindrical shell with FFFF and CCCC boundary conditions, respectively. The material and geometry constants of the layers of the shell are: R = 2 m, L/R = 0.5, h/L = 0.01, θ_0 = 2 arcsin 0.25, E_1 = 60.7 GPa, E_2 = 24.8 GPa, μ_{12} = 0.23, $G_{12} = G_{13} = G_{23}$ = 12 GPa, ρ = 1,700 kg/m^3. It should be noted that the zero frequencies corresponding to the rigid body modes were omitted from the results. Excellent convergence of frequencies can be observed in the table. The convergence of the FFFF solutions is faster than those of CCCC boundary conditions. Numerical results reported by Zhao et al. (2003) by using mesh-free method and CST, Messina and Soldatos (1999a) based on HSDT as well as Qatu and Leissa (1991) based on shallow shell

Table 5.13 Convergence and comparison of frequency parameters $\Omega = \omega L^2/h\sqrt{\rho/E_1}$ of a [−60°/60°/60°/−60°] e-glass/epoxy shallow open cylindrical shell

B.C.	$M \times N$	Mode number					
		1	2	3	4	5	6
FFFF	14 × 14	3.2450	5.5874	8.3715	11.120	12.505	15.272
	15 × 15	3.2448	5.5873	8.3700	11.118	12.502	15.271
	16 × 16	3.2439	5.5872	8.3694	11.117	12.500	15.271
	17 × 17	3.2438	5.5871	8.3681	11.115	12.497	15.270
	18 × 18	3.2430	5.5870	8.3676	11.114	12.496	15.270
	Zhao et al. (2003)	3.3016	5.7328	8.5087	11.133	12.626	15.724
	Messina and Soldatos (1999a)	3.2498	5.5910	8.3873	11.137	12.533	15.328
	Qatu and Leissa (1991)	3.2920	5.7416	8.5412	11.114	12.591	15.696
CCCC	14 × 14	24.510	29.276	36.634	37.998	43.387	46.288
	15 × 15	24.509	29.272	36.623	37.986	43.385	46.278
	16 × 16	24.505	29.255	36.619	37.975	43.384	46.270
	17 × 17	24.504	29.253	36.613	37.968	43.383	46.265
	18 × 18	24.502	29.243	36.610	37.962	43.382	46.261

Table 5.14 Comparison of frequency parameters $\Omega = \omega L^2\sqrt{\rho/E_1 Rh}$ of a [90°/0°] laminated open cylindrical shell with SDSDSDSD boundary conditions (L/R = 5, θ_0 = 60°)

h/R	Method	Mode number					
		1	2	3	4	5	6
0.10	Present	7.025	7.636	8.850	10.84	13.44	14.05
	Messina and Soldatos (1999b)	7.025	7.702	8.932	10.94	13.57	14.05
	Difference (%)	0.01	0.87	0.93	0.97	0.95	0.01
0.05	Present	5.919	8.140	9.934	11.11	14.43	18.01
	Messina and Soldatos (1999b)	5.932	8.153	9.935	11.12	14.45	18.03
	Difference (%)	0.21	0.15	0.01	0.10	0.13	0.13
0.02	Present	5.050	9.777	14.84	15.38	15.71	15.97
	Messina and Soldatos (1999b)	5.049	9.774	14.84	15.40	15.71	16.01
	Difference (%)	0.02	0.03	0.02	0.14	0.02	0.27
0.01	Present	5.724	11.04	12.29	13.03	14.64	17.63
	Messina and Soldatos (1999b)	5.724	11.03	12.27	13.03	14.62	17.61
	Difference (%)	0.00	0.05	0.13	0.04	0.14	0.13

theory are included in Table 5.13. These comparisons show the present solutions are in good agreement with the reference results, although different theories and methods were employed in the literature.

To further validate the accuracy and reliability of current solution, Table 5.14 shows the comparison of frequency parameters $\Omega = \omega L^2\sqrt{\rho/E_1 Rh}$ of a two-layered, cross-ply [90°/0°] open cylindrical shell subjected to SDSDSDSD boundary conditions, with results provided by Messina and Soldatos (1999b) based on the conjunction of Ritz method and the Love-type version of a unified shear-deformable shell theory. The shell parameters used in the comparison are: $E_2 = 25E_2$, R = 1 m, L/R = 5, θ_0 = 60°. The first six frequencies and four sets of thickness-radius ratios, i.e., h/R = 0.1, 0.05, 0.02 and 0.01, corresponding to thick to thin open cylindrical shells are performed in the comparison. It is clearly evident that the present solutions are generally in good agreement with the reference results, although a different shell theory is employed by Messina and Soldatos (1999b). The differences between these two results are very small, and do not exceed 0.97 % for the worst case.

5.4.2 *Laminated Open Cylindrical Shells with General End Conditions*

Some further numerical results for laminated open cylindrical shells with different boundary conditions and shell parameters, such as geometric properties, lamination schemes are given in the subsequent discussions.

Table 5.15 Frequency parameters Ω of a three-layered, cross-ply [0°/90°/0°] open cylindrical shell with various boundary conditions and circumferential included angles (R = 1 m, L/R = 2, h/R = 0.1)

θ_0	Mode	Boundary conditions						
		FFFF	FSFS	FCFC	SFSF	CFCF	SSSS	CCCC
π/4	1	11.203	75.065	88.901	12.815	21.399	78.293	91.804
	2	25.499	77.465	89.414	14.769	22.509	86.921	102.555
	3	31.422	85.618	94.223	39.514	41.030	90.751	102.682
	4	46.947	86.141	99.258	41.021	49.378	95.231	114.025
π/2	1	5.6344	18.757	28.875	13.570	21.848	28.754	39.274
	2	11.724	25.491	32.998	16.635	23.679	45.505	54.963
	3	15.825	41.360	48.575	22.320	27.634	53.806	63.642
	4	27.761	42.306	49.078	37.420	40.797	62.373	72.898
3π/4	1	3.5787	7.1550	12.138	14.598	22.466	26.289	31.315
	2	4.9181	18.335	21.376	15.008	22.664	26.570	34.544
	3	8.3994	19.207	23.673	22.782	28.235	40.285	49.556
	4	13.994	20.658	23.820	26.321	30.282	50.600	59.527
π	1	2.4902	3.1939	6.0606	14.731	22.517	23.135	29.297
	2	2.6064	9.6122	12.938	14.960	22.668	25.209	30.625
	3	5.4335	10.087	13.014	21.990	27.370	31.561	36.692
	4	7.4475	17.262	17.967	23.496	28.851	35.752	43.198
5π4	1	1.5952	1.4971	3.3390	14.805	22.570	22.463	28.530
	2	1.8119	5.5228	7.4940	14.959	22.659	23.343	28.671
	3	3.8722	5.6869	7.8281	21.241	26.976	27.562	34.163
	4	4.4292	11.566	13.214	23.912	28.954	31.578	35.014

Table 5.15 gives the first four frequency parameters Ω of a three-layered, cross-ply [0°/90°/0°] open cylindrical shell with various boundary conditions and circumferential included angles (θ_0). The material properties and geometric dimensions of the shell are: $E_2 = 15E_2$, R = 1 m, L/R = 2, h/R = 0.1. Five different circumferential included angles, i.e., $\theta_0 = \pi/4$, $\pi/2$, $3\pi/4$, π and $5\pi/4$, are considered in the calculation. These results may serve as benchmark values for future researches. It is obvious from the tables that the increase of the circumferential included angle will results in decreases in the frequency parameters. Meanwhile, we can see that an open shell with higher constraining rigidity will have higher vibration frequency parameters. For the sake of enhancing our understanding of vibration behaviors of the open cylindrical and conical shells, the first three mode shapes for the shell with CCCC boundary conditions are present in Fig. 5.15, which is constructed in three-dimension views.

Table 5.16 lists the lowest four frequency parameters Ω for a two-layered, cross-ply [0°/90°] open cylindrical shell with various boundary conditions and thickness-to-radius ratios. The open cylindrical shell under consideration having radius

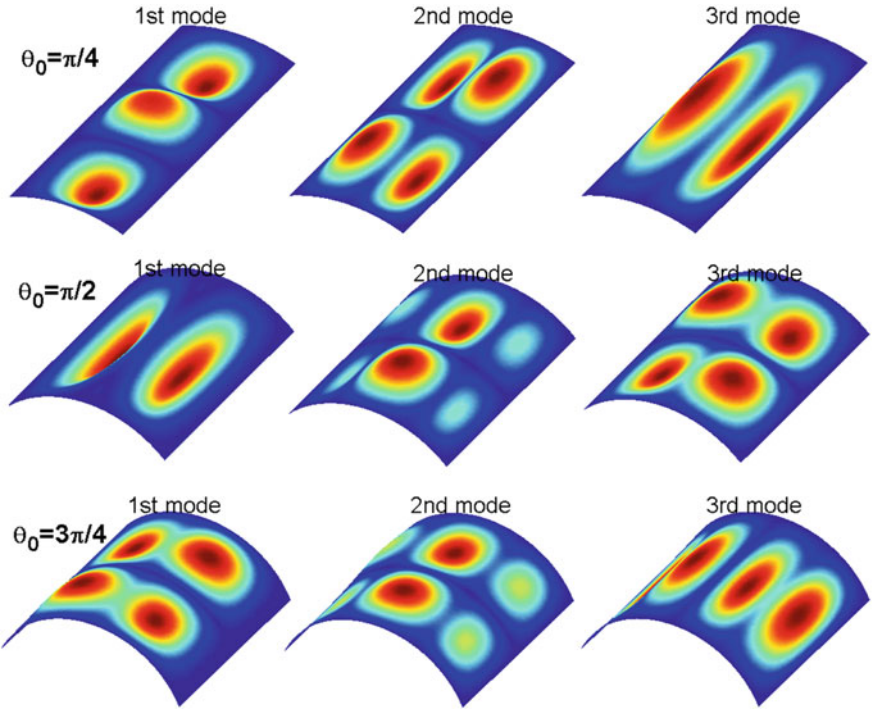

Fig. 5.15 Mode shapes for a CCCC restrained [0°/90°/0°] laminated open cylindrical shell

R = 1 m, length-to-radius ratio of 2 and circumferential included angel of π. Five thickness-to-radius ratios, i.e., h/R = 0.01, 0.02, 0.05, 0.1 and 0.15 are used in the analysis. It is interesting to see that the frequency parameters of the shell decrease with thickness-to-radius ratio increases. Furthermore, by comparing results of the shell with FSFS (or FCFC) boundary conditions with those of SFSF (or CFCF) case, it is obvious that fixation on a curved boundary will results in higher frequency parameters than on a straight boundary.

As the final numerical example, Table 5.17 shows the lowest five frequency parameters Ω of a three-layered [0°/ϑ/0°] open cylindrical shell with different boundary conditions and fiber orientations. Four different lamination schemes, i.e., ϑ = 0°, 30°, 60° and 90° are performed in the calculation. The shell parameters with following material and geometry properties are used in the investigation: R = 1 m, L/R = 2, h/R = 0.05, E_1/E_2 = 15. It is interesting to see that the maximum fundamental frequency parameters for different boundary conditions are obtained at different fiber orientations. For FFFF, FSFS and FCFC boundary conditions, the corresponding maximum fundamental frequency parameters occur at ϑ = 90°. These

Table 5.16 Frequency parameters Ω of a two-layered, cross-ply [0°/90°] open cylindrical shell with various boundary conditions and thickness-to-radius ratios (R = 1 m, L/R = 2, $\theta_0 = \pi$)

h/R	Mode	Boundary conditions						
		FFFF	FSFS	FCFC	SFSF	CFCF	SSSS	CCCC
0.01	1	2.7758	4.8157	9.4618	45.087	46.724	104.38	106.04
	2	3.9626	14.292	20.056	45.222	46.904	105.72	106.88
	3	6.5409	14.680	20.727	79.406	83.653	122.51	129.92
	4	11.292	28.036	34.594	79.608	83.945	129.47	130.07
0.02	1	2.6191	4.7869	9.3262	30.237	32.685	68.450	69.976
	2	3.9162	14.099	19.714	30.366	32.818	69.339	71.337
	3	6.3503	14.556	20.430	55.422	61.528	85.308	92.157
	4	11.239	27.486	33.621	55.517	61.688	91.626	93.121
0.05	1	2.5501	4.6945	9.1067	18.124	21.140	39.402	40.629
	2	3.8715	13.446	18.767	18.410	21.505	39.478	42.805
	3	6.2003	14.126	19.714	35.339	36.116	54.089	59.261
	4	11.057	25.129	29.092	36.435	39.984	58.676	61.573
0.10	1	2.5060	4.5163	8.6298	12.651	15.653	24.724	27.534
	2	3.8048	12.113	16.377	13.299	16.324	27.269	28.391
	3	6.0116	13.250	18.066	21.833	22.930	35.093	39.281
	4	10.663	19.467	19.878	27.237	28.023	42.300	46.914
0.15	1	2.4675	4.3166	8.0369	10.539	13.198	19.651	21.131
	2	3.7283	10.655	13.535	11.002	13.716	20.182	22.567
	3	5.8170	12.279	14.937	17.058	18.066	28.612	32.653
	4	10.188	14.864	16.173	19.937	20.858	32.926	37.089

Table 5.17 Frequency parameters Ω of a three-layered, [0°/ϑ/0°] open cylindrical shell with various boundary conditions and fiber orientations (R = 1 m, L/R = 2, h/R = 0.05)

ϑ	Mode	Boundary conditions						
		FFFF	FSFS	FCFC	SFSF	CFCF	SSSS	CCCC
0°	1	2.1221	2.6128	5.0303	19.047	28.564	32.137	39.663
	2	2.5086	7.9443	10.978	19.186	28.650	33.589	40.141
	3	5.2843	9.1689	11.820	30.775	37.686	39.470	47.388
	4	6.1129	15.962	18.954	32.796	39.484	44.132	50.542
30°	1	2.1451	2.6571	5.1170	21.693	30.077	41.030	47.136
	2	2.7402	8.0809	11.174	21.710	30.089	41.159	47.779
	3	5.6245	9.6128	12.314	38.942	44.967	49.744	55.636
	4	6.2681	16.249	19.961	40.521	46.410	50.257	57.472
60°	1	2.2825	2.9658	5.7048	20.985	29.273	39.105	45.667
	2	2.8505	9.0178	12.470	21.060	29.317	40.405	46.919
	3	5.6029	10.197	13.296	37.684	43.651	48.884	55.513
	4	7.1056	18.165	21.597	38.109	43.870	51.548	59.705
90°	1	2.5305	3.2222	6.2084	19.347	28.270	34.420	41.995
	2	2.6181	9.8038	13.573	19.611	28.430	36.452	42.414
	3	5.5442	10.496	13.889	32.218	38.778	43.661	52.435
	4	7.5371	19.500	22.541	36.199	42.098	51.308	57.262

are obtained at $\vartheta = 30°$ for SFSF, CFCF, SSSS and CCCC boundary conditions. In addition, CFCF yields the minimum fundamental frequency parameter at $\vartheta = 90°$ while it is obtained at $\vartheta = 0°$ for other boundary conditions.